Preprints.org

Article

Major and Trace Elements in Soils from an Industrial Area in the Lower Danube Basin: Levels, Transfer to Crops (Wheat, Corn, Sunflower) and Health Risk

Antoaneta Ene [*] , Sorina Simona Moraru , Dana Iulia Moraru , Ana Pantelica , Steluta Gosav ,
Ceoromila Alina-Mihaela

Article

Major and Trace Elements in Soils from an Industrial Area in the Lower Danube Basin: Levels, Transfer to Crops (Wheat, Corn, Sunflower) and Health Risk

Antoaneta Ene [1,*], Sorina Simona Moraru [1], Dana Iulia Moraru [1,2], Ana Pantelica [3], Steluta Gosav [1] and Alina Mihaela Ceoromila [1,4]

[1] INPOLDE Research Center, Department of Chemistry, Physics and Environment, Faculty of Sciences and Environment, Dunarea de Jos University of Galati, 47 Domneasca St., 800008 Galati, Romania; antoaneta.ene@ugal.ro (A.E.), simoarb@yahoo.com (S.S.M.)

[2] Faculty of Food Science and Engineering, Dunarea de Jos University of Galati, 111 Domneasca St., 800201 Galati, Romania; dana.moraru@ugal.ro

[3] "Horia Hulubei" National Institute for R&D in Physics and Nuclear Engineering, 30 Reactorului St., 077125 Magurele, Ilfov, Romania; apantel@nipne.ro

[4] Cross-Border Faculty, Dunarea de Jos University of Galati, 111 Domneasca St., 800201 Galati, Romania; alina.cantaragiu@ugal.ro

* Correspondence: antoaneta.ene@ugal.ro

Abstract: The study aimed to evaluate for the first time the degree of contamination of soil and crops with major and trace elements (Cd, Co, Cr, Cu, Ni, Pb, Zn, F, Na, Mg, Si, P, Cl, Fe, Al) in agricultural lands situated in the Lower Danube Basin, Galati and Braila counties (SE Romania), impacted by the steel industry. Soil samples from two depths (0–5 cm and 5–30 cm), as well as leaves and seeds of wheat, corn, and sunflower, were collected from 11 different sites. Along with elemental and mineralogical analysis, performed by HR-CS AAS, PIGE, SEM-EDX and ATR-FTIR, the soil pH, texture, organic matter, electric conductivity and $CaCO_3$ content were investigated. The results showed that the levels of Cr (83.270–383.100 mg kg^{-1}), Cu (17.110–68.151 mg kg^{-1}), Ni (30.157–55.656 mg kg^{-1}), and F (319–544 mg kg^{-1}) in soil exceeded the Romanian regulations for sensitive use of the land. The pollution indices (Igeo, EF, PI, PERI) indicate that the soil is moderate to highly contaminated with Cr, Ni and Cu, while CSI and mERM$_Q$ indices suggested a relatively low risk for metal contamination. The concentrations of elements in plant tissues and bioaccumulation factors (BFs) show the soil-plant relation and health risk, but also the elemental selectivity of vegetal compartments. Thus, the results showed that wheat plants tend to exclude the bioaccumulation of certain elements in their tissues, while for Zn and Cu, the bioaccumulation pattern is different. In the case of corn, most BFs were below 1, indicating limited phytoaccumulation capacity. However, exceptions were observed for Cd, Zn, and Cu. Sunflower BFs indicate higher bioconcentration of Cu, Cd, and Zn in both the leaves and seeds compared to other elements. Chromium (Cr) contributes to non-carcinogenic dermal contact and ingestion hazards, with children being more susceptible to the adverse effects of this contaminant.

Keywords: soil; wheat; sunflower; corn; trace elements; pollution; heavy metals; bioaccumulation factor; lower danube basin; health risk

1. Introduction

The responsible and judicious management of soil resources is of paramount importance in maintaining the sustainability of our environment. This includes the utilization of appropriate practices for the preservation and protection of soil health and fertility, while also taking into account the unique characteristics of each specific soil type [Arbanas (Moraru) S.-S., 2022]. The soil is a critical natural resource that plays a vital role in sustaining life on Earth. It serves as an interface between different geospheres and interacts with them to exchange matter and energy. Numerous studies have demonstrated the ecological significance of soil, with edaphic conditions directly influencing the

chemical composition and plants growth [Wang, Y. et al, 2023]; [Blum, W.E.H., 2005]; [Trap, J. et al., 2016]. Soils in proximity to industrial areas, heavily trafficked roads, mines, and waste storage centers are exposed to high levels of elements and toxic chemical compounds. These contaminants can disrupt natural biological processes and may be absorbed by plants, subsequently entering the food chain [Jakubus, M.; Bakinowska, E. 2022], [Costa, C.; Lia, F., 2022], [Zhou, B. et al, 2023], [Zhou, H. et al, 2022]. Furthermore, harmful elements can enter the soil through agricultural products used for fertilization and pest control, posing additional risks to the ecosystem.

The issue of environmental pollution in Galati and Braila counties is a significant concern, particularly due to the industrial activities of the Galati Iron and Steel Plant. Currently, there is limited data on soil contamination with heavy metals caused by steelmaking or other human activities in the Galati-Braila region [Ene, A. et al, 2024]. Regarding the contamination of cultivated plants, vegetables, fruits, and fodder plants with toxic elements discharged from industrial activities, as well as the mismanagement of fertilizers, amendments, and pesticides, there is a lack of specific data for the area under investigation.

The main objective of this study was to examine the extent of soil and crop (wheat, corn, sunflower) contamination with both major and trace elements in the industrial area of Galati metallurgical enterprise. These elements are crucial for supporting life on Earth, but their presence at elevated levels can pose considerable health risks. The study also aimed to determine the elemental bioaccumulation in crop tissues and to assess the contamination level and risk of toxic elements in soils using pollution indices, and the human health hazards associated with ingestion, dermal contact, and inhalation of the toxicants.

2. Materials and Methods

2.1. Study Area

The research was carried out in the south of Galati County and the north of Braila County, southeast of Romania, in some agricultural territories from the Lower Danube Basin which are near the Iron and Steel Plant (I.S.P.) industry (Figure 1) [Arbanas (Moraru) S.-S., 2022].

This area is geographically located in the Covurlui and Siret Plains and is characterized by quaternary loess and loessoid deposits of eolian origin, as well as fluviatile deposits. These deposits are the parent material for the prevalent soil types in this area, namely chernozems and fluvisols.

The steel plant began steel production activity 65 years ago, which led to the neighbouring lands' contamination with toxic elements, mostly heavy metals. Although plant re-engineering has helped in reducing emissions, the irrational use of chemical fertilizers and pesticides still causes significant imbalances in the adjacent agroecosystems.

The sampling sites were located on arable lands, cultivated with the three main crops that have the highest favorability for the researched area, namely wheat (*Triticum vulgare Vill.*), corn (*Zea mays L.*) and sunflower (*Helianthus annuus L.*). Sampling sites position is presented in Table 1.

Table 1. The geographical position of soil sampling sites.

Sample ID	Sampling location	Longitude	Latitude	Altitude (m)
I-1a/1b	E of Sivita	45°36′40.02″	28°03′53.05″	4
I-2a/2b	V of Sivita, Tatarca Hill	45°36′35.00″	28°02′19.00″	97
I-3a/3b	NV of Tulucești, right side of Tartacuta Valley	45°35′08.02″	28°01′35.95″	120
I-4a/4b	NV of Tulucesti, left side of Tartacuta Valley	45°35′11.98″	28°01′56.00″	113
I-5a/5b	NV of Ghilanu Sasa Forest	45°37′29.01″	28°01′08.01″	142
I-6a/6b	Ghilanu Hill	45°37′34.00″	28°01′42.00″	106
II-1a/1b	on the right side of Malina Valley	45°25′05.00″	27°56′36.00″	21
II-2a/2b	between Serbestii Noi and Sendreni villages	45°25′21.33″	27°53′37.05″	28
III-1a/1b	V of Pietroiu	45°19′19.91″	27°52′11.00″	7
III-2a/2b	on the left side of Paslaru Valley	45°23′30.02″	27°54′56.00″	5

| III-3a/3b | on the left side of Sendreni-Baldovinesti road | 45°23'38.62" 27°55'17.90" 5 |
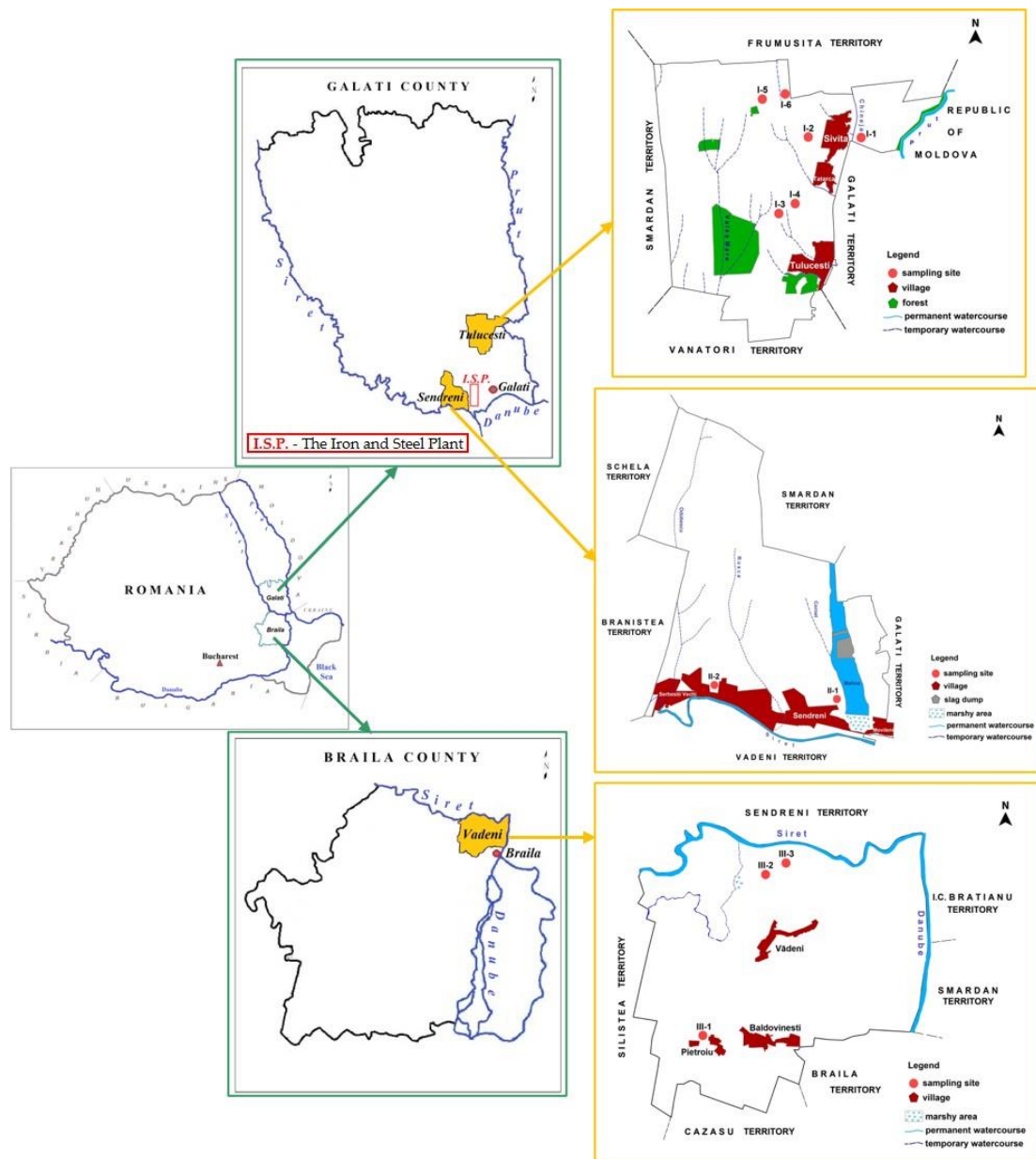
Figure 1. Soil and crops sampling sites in Tulucesti, Sendreni, and Vadeni, Galati-Braila region, SE Romania.

2.2. Soil Sampling and Plants Collection

The soil samples were collected with a stainless-steel knife from pits with a size of 30x30x30 cm by 0-5 cm and 5-30 cm depth according to [Order no. 184/1997] - Figure 2. Each soil sample, weighing approximately 400 g, was carefully stored in a sealed plastic bag and assigned a unique number for identification purposes. To avoid any contamination from the top layer, the samples were collected from the bottom up. Prior to sampling, the depths were defined and the excavation site was refreshed.

4

Figure 2. Soil sampling pits.

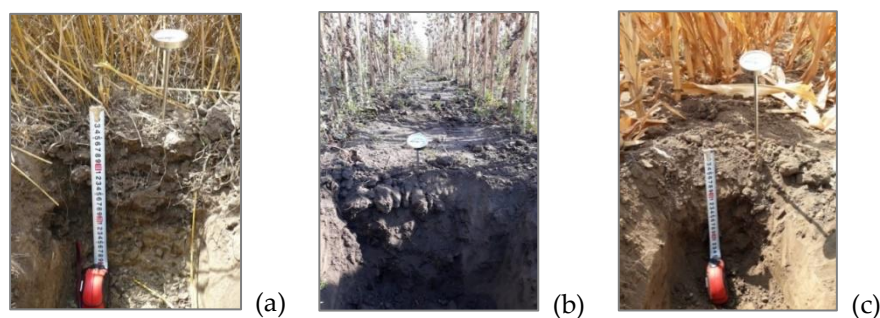The crop samples consisted of mature and healthy wheat (*Triticum Vulgare* Vill.), corn (*Zea mays* L.), and sunflower (*Helianthus annuus* L.) plants from the same lots where the soils were taken. The sampling process was carried out following the guidelines provided by [Benton Jones Jr., J., 1998]. During the sampling process, plants located at the ends of the lots and visibly affected ones were excluded.

2.3. Soil and Plants Analysis

The soil samples were cleaned of root, stones and other debris, air-dried, crushed in a porcelain mortar and sieved through a 150 μm nylon mesh according to [SR ISO 11466:1999].

The crop samples were first sorted into leaves and grains, and then washed with tap water and rinsed with distilled water to remove any dust and pesticides that might have been present. The washing process was quick to prevent any loss of chemical elements. After air-drying in a contamination-free room with good ventilation, the plants were further dried in an oven at 80°C until they reached a constant weight (Figure 3). Once dried, samples were then crushed in a porcelain mortar, sifted through a 150 μm nylon mesh, and stored in plastic bags in a desiccator until the analysis.
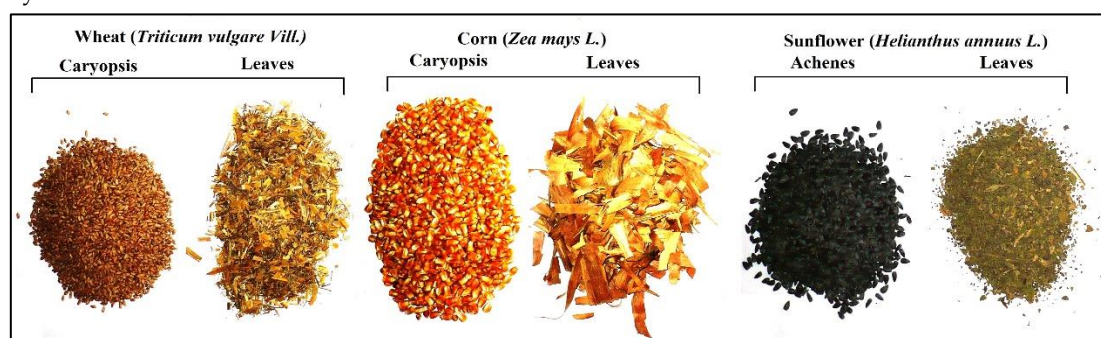
Figure 3. Crop grains/seeds and leaves samples after cleaning and drying.

For various analyses, the soil and plant samples were pelletized using the Specac manual hydraulic press 15 Ton and its mould. 0.5 tons of force were applied for soil samples and 4 tons of force for plant samples. However, sunflower seeds, which contain oil, could not be pelletized. Therefore, they were analyzed at the surface and in section.   Several methods were used to investigate the soil and plant, in order to determine their chemical properties. The pH was measured according to [SR 7184/13:2001], organic matter (OM) and organic carbon (OC) levels were determined using [STAS 7184/21-82]. The $CaCO_3$ content was measured by the volumetric method according to [SR EN ISO 10693: 2014], while the sum of exchange bases (SEB), hydrolytic acidity (HA), and degree of base saturation (DBS) were examined as per [Borlan, Z. and Rauta, C., 1981]. To determine the electrical conductivity (EC) and total content of soluble salts (TDS), [SR ISO 11265 + A1: 1998] and [STAS 7184/7-87] were used. The soil granulometric fractions were employed according to [STAS 7184/10-79].

Moreover, advanced complementary methods were applied at INPOLDE research center of Dunarea de Jos University of Galati and "Horia Hulubei" National Institute for R&D in Physics and Nuclear Engineering (NIPNE) at Magurele, Romania, to study the soil and plant. The mineralogical and elemental analysis were conducted by Scanning Electron Microscopy combined with Energy-Dispersive X-ray analysis (SEM-EDX) and the Attenuated-Total Reflectance-Fourier Transform Infrared technique (ATR-FTIR). The High-Resolution Continuum Source Atomic Absorption Spectrometry (HR-CS AAS) method was employed to determine toxic and potential toxic metals, such as Cd, Co, Cr, Cu, Ni, Pb, Zn, Mn. The non-destructive Particle-Induced Gamma-ray Emission (PIGE) nuclear technique was useful to identify heavy and light elements like Ca, Ti, Cr, Mn, Fe, Ni, Zn, Na, Mg, Al, Si, P, S.

For the determination of the total contents of heavy metals in soil and plant the following protocols were applied: *for soil.* Soil samples were prepared as described above and oven-dried at 105°C until a constant mass was achieved, as per [SR ISO 11465:1998]. Around 1 g of each sample was treated with modified aqua regia, which is a mixture of 2.5 ml HNO_3 (69%), 7.5 ml HCl (37%), and 1 ml HF (48%). A control sample was also prepared using the same reagent mixture. The prepared samples were placed in a Berghof microwave oven and digested as follows: Step 1 - 180ºC, time 15', power 90 %, Step 2 - 150ºC, time 15', power 90 %, Step 3 - 100ºC, time 10', power 90 %. After cooling to room temperature for about 30 minutes, the digestate was filtered, transferred to 50 ml volumetric flasks, and diluted with 0.5% HNO_3. *for plant.* Approximately 0.3 g of finely ground and dried plant samples were placed in reaction vessels. Then, 6 ml of HNO_3 (69%) was added to the vessels and left overnight under a fume hood. The following day, 3 ml of H_2O_2 (35%) was added to the teflon vessels. For comparison, a control sample was also prepared using the same reagent mixture. The digestion vessels were placed in the Berghof microwave oven and a four-step digestion program was used as follows: Step 1 - 140ºC, time 10', power 90 %, Step 2 - 180ºC, time 15', power 90 %, Step 3 - 100ºC, time 15', power 90 %, Step 4 - 85ºC, time 5', power 90 %. After cooling at room temperature, the digested samples were transferred to 50 ml volumetric flasks and then diluted with 0.5% HNO_3. A ContrAA 700 Analytik Jena spectrometer was used to investigate the concentration of heavy metals in soil and plants employing both flame and graphite oven methods.

The mineralogical composition of soil and chemical groups in plant structures were analyzed using the ATR-FTIR method, with assistance from a Bruker Tensor 27 FTIR spectrometer that featured an ATR unit coupled with a diamond crystal. Soil and plant samples, prepared as described, were put as a thin layer onto the ATR device. Background correction was performed, and spectra were recorded as an average of 32 scans per analyzed sample within the range of 4000-400 cm^{-1} and at a resolution of 4 cm^{-1}. To separate overlapping absorption bands between 1250-850 cm^{-1} in soil samples, deconvolution of ATR-FTIR spectra was conducted using OriginPro 2016 software, version 9.3.226.

The Scanning Electron Microscopy (SEM) method was used to analyze soil and plant samples to study their microstructure and surface morphology. The SEM images were captured using an SEM microscope, model FEI QUANTA 200, Thermo Fisher Scientific, USA. During imaging investigations, the electron beam was accelerated to an accelerating voltage of 20 kV, which was sufficient to obtain a secondary electron signal resulting from the excitation of as many constituent chemical elements as possible. The vacuum pressure was set to 60 Pa (medium vacuum), and the working distance was 10 mm. SEM images were taken at various magnifications, ranging from 250X (overview) to 5000X (structural details).

For the SEM analysis, the samples were mounted on an aluminum support using double-adhesive carbon tape, following the protocol by [Caprita, F.-C. et al, 2021]. Since the samples were dried, finely mortared, and pastilled, it was necessary to cover them with a thin layer of gold before the microscopic analysis. The surface metallization step was performed using SPI Sputter Coater Module equipment (SPI Supplies, USA) at a pressure of 6 mbar and plasma current intensity of 18 mA, resulting in a metal layer with a thickness of 10 nm.

The SEM micrographs were complemented by the X-ray spectra through a semi-quantitative elemental analysis of the samples using the Energy Dispersive X-ray Spectroscopy (EDX) method.

This required the use of a Si (Li) detector, coupled to the SEM microscope. Four different micro areas were randomly selected and analyzed on a surface with an area of 60 μm2, calculating the average value of the percentage concentration of the elements. EDX spectra were recorded at a magnification of 5,000X, and the measurement time was 100 sec. To eliminate the matrix effect, the ZAF correction algorithm was applied (correction by atomic number (Z), absorbance (A), and fluorescence (F)), as suggested by [Caprita, F.-C. et al, 2021]. The algorithm converted the apparent concentrations (raw spectral line intensity) into semi-quantitative concentrations.

The PIGE technique used a proton beam with an energy of 3 MeV to irradiate environmental samples in a multi-target reaction chamber under vacuum. An Ortec HPGe detector (GEM10PA-70) with a relative efficiency of 10% and a resolution of 1.75 keV at 1332 keV (60Co) was used in the experimental setup. The detector was positioned at a 45° angle to the beam path and the target sample. The finely grounded, homogenized, and pressed samples were fixed on a target holder and introduced into the reaction chamber for vacuum dosing of the elements.

The specialized software was used to configure the operating parameters, such as irradiation time (1200 s for soil and 2700 s for plants) and fixing the beam trajectory. Two measurements were taken for each soil/plant sample.

The data was processed using the SRIM software. The results obtained through the PIGE method were quantified by establishing a ratio between the elemental concentration of a reference material and the mass of fractions from a matrix similar to the analyzed material. To achieve this, certified reference materials, namely INCT-TL-1 (Tea Leaves), INCT-OBTL-5 (Oriental Basma Tobacco Leaves), IAEA-356, and IAEA SD-M-2/TM (Marine Sediment) were used.

2.4. Pollution and Health Risk Assessment

In recent decades, pollution indices have become increasingly valuable in evaluating the degree of soil and sediment contamination [Wang, C. et al, 2024], [Wu, C. et al, 2024], [Jaskuła, J. et al, 2021], [Dou, C. et al, 2023], [Yang, L.-Y. et al, 2024]. These indices provide crucial information about the origin of the contamination, whether it is natural, anthropogenic, or a combination of both. Additionally, they offer insights into the associated risks posed to the environment and human health.

Different pollution indices have been used to evaluate the extent of soil contamination by toxic elements. These include the *Geoaccumulation Index* (Igeo), *Enrichment Factor* (EF), *Single Pollution Index* (PI), the *Potential Ecological Risk Index* (PERI), the *Contamination Severity index* (CSI), and the *mean Effect Range Median quotient* (mERM$_Q$). These indices provide varying perspectives on the nature and degree of contamination, offering a comprehensive understanding of the contamination state of soil in the given area. The data generated can be useful in making decisions on land use and remediation efforts. The indices were calculated and evaluated according to [Ahmed F. et al. 2016], [Caeiro S., 2005], [Sutherland, R.A., 2000], [Awadh, S.M. and Al-Hamdani, J.A.JM.Z., 2019], and [Kowalska, J.B. et al, 2018].

The Geoaccumulation Index (Igeo), first introduced by [Műller G., 1969], is the ratio of the concentration of heavy metals in soil to their natural geochemical background-Eq. (1)

$$\text{Igeo} = \log_2\left[\frac{C_i}{1{,}5{\cdot}B_i}\right] \tag{1}$$

where *Ci* refers to the concentration of a particular *i* metal in the soil (mg kg^{-1}), and *Bi* refers to the concentration of that same metal in the natural background (mg kg^{-1}). The constant 1.5 is used to facilitate accurate and consistent data analysis, while also minimizing the impact of lithological variations on the overall results. Soil contamination degree was classified according to the scale of interpretation developed by Müller G. as follows: Igeo ≤ 0-unpolluted (Class 0), 0 < Igeo ≤ 1-unpolluted to moderate polluted (Class 1), 1 < Igeo ≤ 2-moderate polluted (Class 2), 2 < Igeo ≤ 3-moderate to high polluted (Class 3), 3 < Igeo ≤ 4-high polluted (Class 4), 4 < Igeo ≤ 5 - high to very high polluted (Class 5), > 5-excesively polluted (Class 6).

The *Enrichment Factor* (EF), first calculated by Buat-Menard P. and Chesselet R. in 1979 [Nikolaidis, C. et al, 2010] is an index that helps to assess the impact of human activities on the

concentration of metals in soil. It is calculated by dividing the concentration of a particular metal in the soil by the concentration of a naturally occurring element such as Fe, Al, Sc, Mn, or Zr, which remains constant over time. In this study, the element Al was used as a reference to normalize the metals enrichment (Eq. (2)).

$$\text{EF}_i = (C_i/C_{Al})/(B_i/B_{Al}) \tag{2}$$

where C_i refers to the concentration of the metal i in soil (mg kg^{-1}), C_{Al} is the concentration of aluminium in soil, B_i is the concentration of that same metal in the natural background (mg kg^{-1}), and B_{Al} - is the concentration of Al in the natural background. The results were classified by [Sutherland, R.A., 2000] classes of interpretation: Class 1: <2 - deficiency - minimal enrichment (unpolluted soil - low polluted soil), Class 2: 2-5 - moderately enrichment (moderately polluted soil), Class 3: 5-20 - significant enrichment (significant polluted soil), Class 4: 20-40 - high enrichment (high polluted soil), Class 5: > 40 - extremely high enrichment (extremely polluted soil).

The *Single Pollution Index* (PI), introduced by Wedepohl, K. H. in 1961, is used to identify the metal with the highest impact on environment and it was calculated according to Eq. 3 [Awadh, S.M., Al-Hamdani, J.A.JM.Z., 2019].

$$\text{PI}_i = \frac{C_i}{B_i} \tag{3}$$

where C_i refers to the concentration of the metal i in soil, and B_i is the concentration of that same metal in the natural background, both expressed in mg kg^{-1}. Soil contamination was classified as follows: PI<1 - uncontaminated (Class 1), 1<PI$_i$<2 - low contaminated (Class 2), 2<PI$_i$<3 - moderate contaminated (Class 3), 3<PI$_i$<5 - high contaminated (Class 4), PI$_i$>5 - very high contaminated (Class 5) [Kowalska, J.B. et al, 2018].

The *Potential Ecological Risk Index* (PERI), introduced by Håkanson L. in 1980, expresses the probability of the occurrence of an ecological risk due to contamination with toxic or potentially toxic elements. This index was calculated with [Håkanson L., 1980] formula (Eq. (4)) and its values are classified after the following scale of interpretation: low potential ecological risk (PERI <150), moderate potential ecological risk (150≤ PERI <300), high potential ecological risk (300≤ PERI <600), very high potential ecological risk (PERI ≥600).

$$PERI = \sum_{i=1}^{n} E_r^{\,i} \tag{4}$$

where n is the number of elements, E_r^i is the potential ecological risk of the metal i which is calculated with the Eq. (5).

$$E_r^{\,i} = T_r^{\,i} \cdot PI_i \tag{5}$$

where T_r^i is the toxic response caused by the exposure of the metal i. According to [Håkanson L., 1980], T_r^i values (mg kg^{-1}) are as follows: T_r^{Cd}-30, T_r^{Cu}-5, T_r^{Pb}-5, T_r^{Cr}-2, T_r^{Zn} - 2, T_r^{Ni}-5. According with [Kowalska, J.B. et al, 2018] ecological risk can be classified as follows: low ecological risk (E_r^i < 40), medium ecological risk (40 < E_r^i < 80), considerable ecological risk (80 < E_r^i < 160), high ecological risk (160 < E_r^i < 320), and very high ecological risk (Eri > 320).

The *Contamination Severity index* (CSI), developed by [Pejman A. et al, 2015], was calculated using the formula provided by [El-Alfy, M.A. et al, 2020] and [Kowalska, J.B. et al, 2018] to assess the degree of soil pollution with heavy metals (Eq. (6)).

$$CSI = \sum_{i=1}^{n} W_t \left[\left(\frac{C_i}{ERL_i}\right)^{\frac{1}{2}} + \left(\frac{C_i}{ERM_i}\right)^{2} \right] \tag{6}$$

where W_t is the calculated weight of the metal, C_i refers to the concentration of the metal i in soil, ERL$_i$ represent the value at which the impact on living organisms of the metal is low, while ERM$_i$ is the value at which the impact on living organisms of the metal is medium. Table 2 displays the heavy metals weight values, as well as ERM$_i$ and ERL$_i$ values.

Table 2. Heavy metals weight, ERMi and ERLi values.

Metal	W_t [Kowalska, J.B. et al, 2018]	ERL_i [Long, E.R. et al, 1995]	ERM_i [Long, E.R. et al, 1995]
Cu	0.075	34	270
Zn	0.075	150	410
Cr	0.134	81	370
Ni	0.215	20.9	51.6
Pb	0.251	46.7	218
Cd	0.250	1.2	9.6

The classification of soil contamination into contamination classes, as per the CSI, is based on the contamination intensity classes defined by [Kowalska, J.B. et al, 2018]. These classes serve as an indicator of the severity of soil pollution present within a given area. The classes are defined as follows: Class 1 (<0.5)-uncontaminated soil, Class 2 (0.5-1.0)-very low level of soil contamination, Class 3 (1.0-1.5)-low level of soil contamination, Class 4 (1.5-2.0)-low to moderate level of soil contamination, Class 5 (2.0-2.5)-moderate level of soil contamination, Class 6 (2.5-3.0)-moderate to strong level of soil contamination, Class 7 (3.0-4.0)-high level of soil contamination, Class 8 (4.0-5.0)-very high level of soil contamination, and Class 9 (>5.0)-excessive level of pollution.

The *mean Effect Range Median quotient* (mERM$_Q$) was calculated according to [El-Alfy, M.A. ş. a., 2020] as Eq. (7).

$$mERM_Q = \frac{\sum_{i=1}^{n} \frac{C_i}{ERM_i}}{n} \qquad (7)$$

where *Ci* refers to the concentration of the metal *i* in soil, *ERMi* is the value at which the impact on living organisms of the metal is medium, and *n* is the number of elements. mERM$_Q$ is classified into four grades: ≤0.1 - low risk, probability of toxicity is 9 %, 0.,1-0.5 - medium risk, probability of toxicity is 21 %, 0.5-1.5 - high risk, probability of toxicity is 49 % şi >1,5 - very high risk, probability of toxicity is 76 % [El-Alfy, M.A. ş. a., 2020].

Plant Bioaccumulation of Major and Trace Elements

To assesss the environmental risk of chemicals, the bioaccumulation factor (BFi) of major and trace elements was calculated according to Eq. (8), as it helps to determine the potential for the toxic or potential toxic elements to accumulate in the food chain and ultimately affect human and animal health.

$$BF_i = \frac{Ci\ plant}{Ci\ soil} \qquad (8)$$

where C$_i$ *plant* refers to the concentration of the element *i* in plant section (leaf and grain) and C$_i$ *soil* is the concentration of the element *i* in soil (mg kg^{-1} d.w.). A BFi>1 indicates that the plant has a higher potential to accumulate the element (the plant is called "accumulator"), while a 1<BFi suggests that the plant is less likely to accumulate the element (the plant is called "excluder") and when BFi=1 it indicates the soil metal contents (the plant is called "indicator") [Olowoyo, J.O. et al, 2010], [Mirecki, N. et al, 2015].

Human health risk assessment is a very important process that involves assessing the potential impact of a hazard on the health of people, and even the comunities they belong to. Due to agricultural practices that cause environmental damage (especially the irrational use of chemical fertilizer, pesticides, amendments, mismanagement of agricultural land use, the lack of tree planting to optimize soil protection against water and wind erosion by which a large amount of dust full of toxicants is released into the air and body of water) and industrial activities, which releases polluting particles into the atmosphere, in the Lower Danube Basin, heavy metals and other contaminants exposure is an actual concern. The dust dispersed from the surface of the agricultural soils in the vicinity of the villages of Tulucesti and Sendreni, from Galati county, and Vadeni, from Braila county,

are thus inhaled, swallowed or even deposited on the surface of the skin, generating health risks for the inhabitants, children being the most exposed. For the study area, there is less information about soil and crop contamination with toxic or potentially toxic elements, and less is known about the non-carcinogenic and carcinogenic risk to which the population of adults and children is exposed during their lifetime.

To assess the potential health risk of contaminants, the analytical data for soil elemental composition (Csoil) and also the reference values and equations given by [USEPA, 2019], [Sarva, M.P. et al, 2018] and [Ackah, M., 2019] were used (see Eq. (9), (10), and (11)).

The Chronic Daily Intake (CDI) for toxic elements exposure is estimated by the CDI for ingestion (CDI$_{ingestion}$), dermal contact (CDI$_{dermal}$), and inhalation (CDI$_{inhalation}$). The equations employed in this regard are as follows:

$$\text{CDI}_{\text{ingestion}} = \frac{Csoil \ x \ IngR \ x \ EF \ x \ ED}{BW \ x \ AT} \ xCF \tag{9}$$

$$\text{CDI}_{\text{dermal}} = \frac{Csoil \ x \ SA \ x \ AF \ x \ ABS \ x \ EF \ x \ ED}{BW \ x \ AT} \ xCF \tag{10}$$

$$\text{CDI}_{inhalation} = \frac{Csoil \ x \ InhR \ x \ ET \ x \ ED}{PEF \ x \ BW \ x \ AT} \tag{11}$$

The parameters of non-carcinogenic and carcinogenic health risk and their reference values are presented in Table 3.

Table 3. Exposure parameters used to assess non-carcinogenic and carcinogenic health risk.

Parameter		Unit	Residential		References
			Adult	Children	
BW	body weight	kg	80	15	USEPA, 2019
ATnc	averaging time for noncarcinogens	days	365x20	365x6	USEPA, 2019
ATc	averaging time for carcinogens	days	25550	25550	USEPA, 2019
IngR	ingestion rate of soil	mg kg^{-1}	100	200	USEPA, 2019
EF	exposure frequency	days years^{-1}	350	350	USEPA, 2019
ED	exposure duration	year	20	6	USEPA, 2019
CF	conversion factor	kg mg^{-1}	10^{-6}	10^{-6}	Sarva, M.P. et al, 2018
SA	skin exposed area	cm^2	6032	2373	USEPA, 2019
AF	soil-to-skin adherence factor	mg cm^{-2}	0.07	0.2	USEPA, 2019
ABS	absorbtion factor				
ABS$_{Cd}$	absorbtion factor for Cd	unitless	0.01	0.01	USEPA, 2015
ABS$_{om}$	absorbtion factor for other metals		0.001	0.001	
InhR	inhalation rate	m^3 day^{-1}	20	10	USEPA, 2019
ET	exposure time	hours day^{-1}	24	24	USEPA, 2019
PEF	particle emission factor	m^3 kg^{-1}	1.36x10^9	1.36x10^9	USEPA, 2019

The Hazard Quotient (HQ$_i$) provides information on the non-carcinogenic risk of element i through chronic daily intake of toxic elements (CDI) relative to the chronic reference dose of the element i (RfD$_i$, mg kg^{-1} day^{-1}) - Eq. (12).

$$\text{HQ}_i = \frac{CDI}{RfD_i} \tag{12}$$

The RfD$_i$ reference values were considered according to [Zeng, X. et al, 2015] as fallows: RfDingestion - Cd (1.00x10^{-3}), Cr (3.00x10^{-3}), Ni (2.00x10^{-2}), Co (3.00x10^{-4}), Cu (4.00x10^{-2}), Pb (3.50x10^{-3}), Zn (3.00x10^{-1}); RfDdermal - Cd (1.00x10^{-5}), Cr (6.00x10^{-5}), Ni (5.40x10^{-3}), Co (1.60x10^{-2}), Cu (1.20x10^{-2}), Pb (5.25x10^{-4}), Zn (6.00x10^{-2}); RfDinhalation - Cd (1.00x10^{-3}), Cr (2.86x10^{-5}), Ni (2.06x10^{-2}), Co (5.71x10^{-6}), Cu (4.02x10^{-2}), Pb (3.52x10^{-3}), Zn (3.00x10^{-1}).

When the hazard quotient (HQ) is greater than 1, it indicates that the exposed individuals are likely to experience adverse health effects. Conversely, when the HQ is less than 1, it suggests that there is no health risk for the exposed individuals [Ackah, M., 2019].

The potential non-carcinogenic risk effects that may occur were investigated by Hazard Index (HI) by Eq. (13).

$$\text{HI} = \sum HQ_i \tag{13}$$

When the HI is greater than 1, it indicates a higher likelihood of a toxicological response to the exposure of harmful substances through multiple pathways. Conversely, a HI score below 1 suggests a low probability of a toxicological response to the combined harmful exposure [Ackah, M., 2019], [Praveena, S.M. et al, 2017].

3. Results and Discussion

3.1. Assessment of Soil Main Parameters Which Influence Elemental Bioavailability

The main soil parameters involved in the absorption and circulation of nutrients and toxic or potentially toxic substances in the soil and from the soil to plants, as well as for the role they play in the development of biological processes, are: pH, $CaCO_3$ content, the sum of exchange bases (SEB), hydrolytic acidity (HA), degree of base saturation (DBS), organic matter (OM), organic carbon (OC), content of total dissolved salts (TDS), and soil texture. Soil main properties of the investigated soils are presented in Table 4. The role of soil parameters in retaining and releasing nutrients and harmful elements is widely recognized. Humus, a vital component for soil fertility, enhances soil structure and water retention, directly impacting the availability of nutrients [Slaboch, J. and Maly, M., 2023]. The soil's pH plays a crucial role in plant development, influencing nutrient uptake and the movement of both toxic and non-toxic metal ions [Zhang, Z. et al, 2023], [Xu, F. et al, 2020], [Adamczyk-Szabela, D.; Wolf, W.M., 2022]. Even at low concentrations, dissolved salts can hinder plant growth and nutrient absorption. Furthermore, the distribution of sand, silt, and clay in the soil affects the absorption and availability of major and minor chemical elements. Each soil texture type possesses unique water retention and nutrient-holding capacities. [Pikuła, D.; Stępień, W., 2021], [Ahmad, I. et al, 2021].

Table 4. Physico-chemical properties of surface soil in the Lower Danube Basin (Tulucesti, Sendreni, Vadeni area) (after [Arbanas (Moraru) S.-S. 2022], [Arbanas (Moraru), S.S. and Ene, A., 2020]).

Sampling site	Layer (cm)	pH	CaCO₃	OM	OC	SEB	HA	DBS	EC	TDS	Clay	Silt	Sand
			(%)			me 100 g soil⁻¹	(%)	(%)	(µS cm⁻¹)	(mg 100 g soil⁻¹)	(%)		
T-1a	0-5	8.35	6.61	3.98	2.31	91.85	0.59	99.36	331.00	112.50	5.57	32.23	62.20
T-1b	5-30	8.48	7.42	3.04	1.76	94.56	0.38	99.60	312.00	106.10	5.62	30.78	63.60
T-2a	0-5	8.16	2.75	3.39	1.97	68.18	0.67	99.03	171.50	58.30	2.87	35.48	61.65
T-2b	5-30	8.06	3.03	3.37	1.95	67.80	0.75	98.91	184.60	52.80	2.48	30.11	67.41
T-3a	0-5	7.44	0.00	2.22	1.29	27.06	1.22	95.69	92.40	31.40	1.30	23.70	75.00
T-3b	5-30	7.59	0.00	1.99	1.15	24.34	1.09	95.71	90.60	30.80	1.40	30.60	68.00
T-4a	0-5	8.32	10.70	1.60	0.93	94.18	0.59	99.38	182.40	62.00	1.57	30.91	67.52
T-4b	5-30	8.40	11.42	1.82	1.06	96.12	0.54	99.44	169.20	57.50	2.15	30.14	67.71
T-5a	0-5	6.63	0.00	2.42	1.40	26.28	2.01	92.90	162.50	55.30	7.70	32.70	59.60
T-5b	5-30	6.56	0.00	2.50	1.45	25.50	2.22	91.99	151.80	51.60	1.20	23.00	75.80
T-6a	0-5	8.32	5.27	2.04	1.18	94.96	0.59	99.38	156.30	53.10	0.84	26.29	72.87
T-6b	5-30	8.31	4.95	1.70	0.99	96.12	0.59	99.39	168.80	57.40	1.27	23.67	75.06
S-1a	0-5	8.40	8.85	2.14	1.24	92.24	0.54	99.42	200.00	68.00	1.31	27.54	71.15
S-1b	5-30	8.47	8.55	1.00	0.58	94.18	0.38	99.60	178.60	60.70	0.99	19.90	79.11
S-2a	0-5	8.39	8.48	1.68	0.97	94.18	0.54	99.43	266.00	90.40	2.40	33.11	64.49

S-2b	5-30	8.59	9.85	1.59	0.92	93.79	0.29	99.69	229.00	77.90	1.00	35.27 63.73
V-1a	0-5	8.13	2.52	2.61	1.51	62.75	0.71	98.88	206.00	70.00	7.28	3.90 88.82
V-1b	5-30	8.15	2.59	1.93	1.12	59.65	0.67	98.89	159.40	54.20	1.43	10.27 88.30
V-2a	0-5	8.30	5.92	2.08	1.21	96.51	0.63	99.35	179.10	60.90	3.08	35.82 61.10
V-2b	5-30	8.38	6.12	2.25	1.31	95.34	0.54	99.44	170.10	57.80	4.69	36.32 58.99
V-3a	0-5	8.44	4.84	1.61	0.93	96.12	0.46	99.52	150.00	51.00	3.89	28.37 67.74
V-3b	5-30	8.47	4.82	1.73	1.00	93.40	0.38	99.59	141.90	48.20	1.57	26.69 71.74

The soils' pH showed a similar distribution on both layers and on the three assessed territories. Generally, the pH is slightly alkaline, ranging between 7.44-8.44 on the 0-5 cm layer and 7.59-8.48 on the 5-30 cm layer. However, the site T-5a/5b is an exception, where the pH is slightly acidic, measuring 6.63 on the 0-5 cm layer and 6.56 on the 5-30 cm layer. The CaCO$_3$ level in the top 30 cm of soil varies from medium to high, ranging between 2.52% and 11.42. In the sites T-3a/3b and T-5a/5b, where the pH is the lowest, CaCO$_3$ is absent. The organic matter (OM) and organic carbon (OC) content levels are impacted by the distribution of granulometric fraction. The OM levels vary from low to high, ranging between 1.61% and 3.98% at 0-5 cm, and between 1.00% and 3.37% at 5-30 cm. The SEB values recorded from 68.18 to 96.51 me 100 g soil^{-1} in the 0-5 cm layer, and 59.65 to 95.34 me 100 g soil^{-1} in the 5-30 cm layer. Meanwhile, the AH values were very low, with measurements ranging between 0.43 and 1.22 me 100 g soil^{-1} in the 0-5 cm layer, and 0.38 and 1.09 me 100 g soil^{-1} in the 5-30 cm layer. The only exception was the T-5b site, where the AH value was 2.22 me 100 g soil^{-1}. Overall, the soil showed a high degree of base saturation, with DBS values ranging from 99.03% to 99.52% in the first 5 cm layer, and from 91.99% to 99.60% in the 5-30 cm layer. Additionally, we evaluated the EC and TDS, which indicated that the soils were generally unsalinized, with the exception of soil samples from the T-1a/1b site located in the Prut meadow, which overlaps alluvial deposits (Table 4).

The soil is classified predominantly as coarse due to the high percentage of sand in comparison with clay and silt. The soil texture distribution is as follows: medium sandy loam (T-1a, T1-b), fine sandy loam (T-5a), fine sand (T-2a, T-2b, T-3a, T-3b, T-4a, T-4b, T-5b, S-1a, S-1b, V-3a, V-3b), medium sand (T-6a, T-6b, V-a, V-1b), sandy silt (S-2a, S-2b, V-2a, V-2b). These textural classes were also identified by [Moraru, S.-S. et al, 2020] for this region.

3.2. Major and Trace Elements Assessment in Soil

Soil levels of contamination in the top layer's sections of 0-5 cm and 5-30 cm is illustrated by Figure 4.
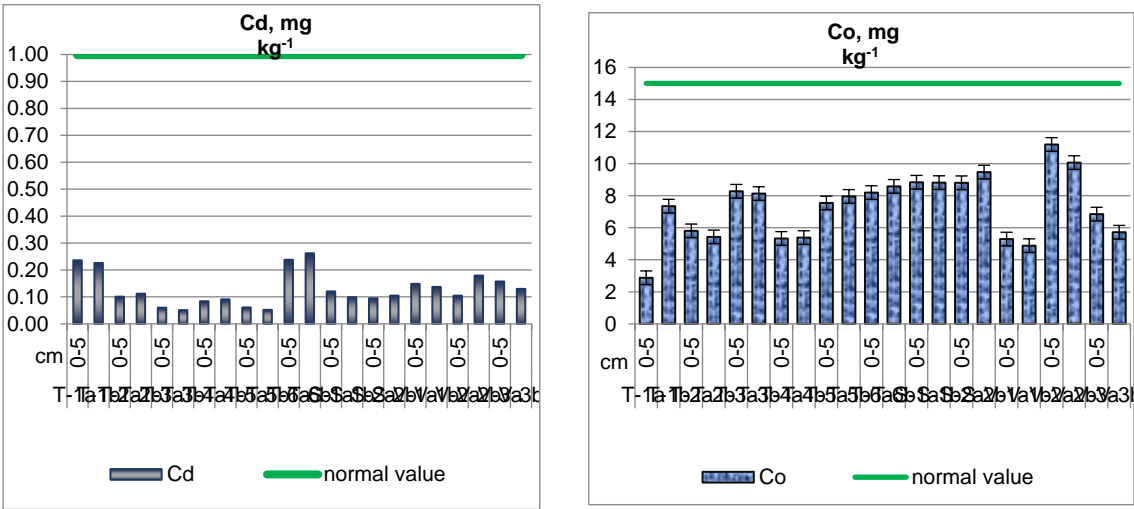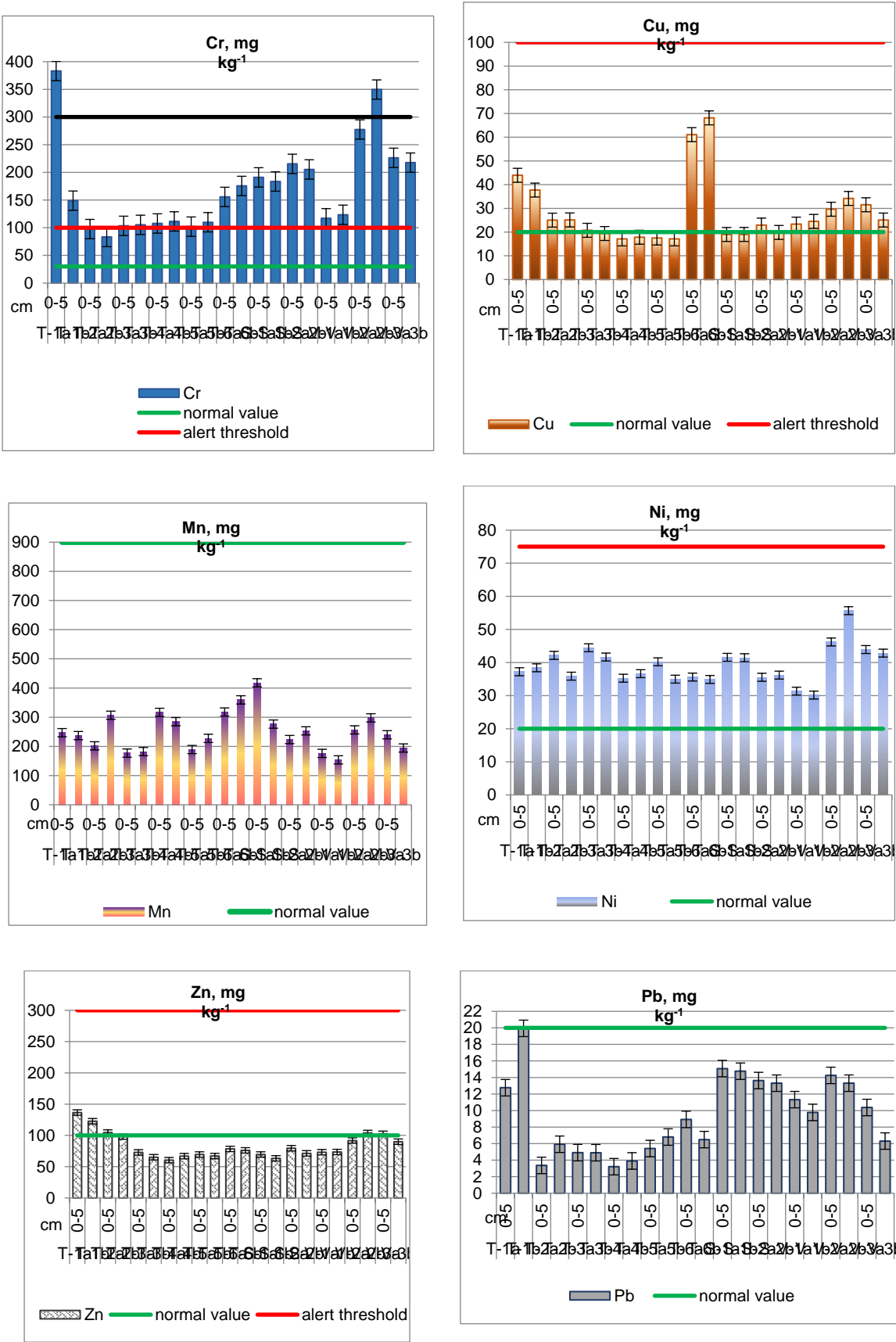
Figure 4. Heavy metals distribution in the upper layer, up to 30 cm, of agricultural soils from the Lower Danube Basin (T-Tulucesti, S-Sendreni, V-Vadeni).

The results were compared with the average values of major and trace elements presented in Table 5, synthesized after [Kabata-Pendias, A., 2011], [Salminen, R. ș. a., 2005], [Dumitru, M. et al,

2011], [Manea, A. et al, 2018], [Pantelica, A. et al., 2013], [Order no. 756/1997] and [Cullen, J.T. and Maldonado, M.T., 2013].

Table 5. Average values of major and trace elements in the upper layer of Continental Crust, World, European and Romanian Soils after various authors and the Ministry of Water, Forests and Environmental Protection of Romania [Arbanas (Moraru) S.-S. 2022].

References	Cd	Co	Cr	Cu	Mn	Ni	Pb	Zn	F	Cl	Ti	Si	Na	Mg	Fe
	(mg kg^{-1})											(%)			
Continental crust [Kabata-Pendias, A., 2011]	0.08*-0.10	10	100	55	900	20	15	70	625	640	4400	-	-	-	5
World soils [Kabata-Pendias, A., 2011]	0.06*-0.41	11.3	59.5	38.9	488	29	27	70	321	300	7038	-	-	-	3.5
European soils[1] [Salminen, R. et al, 2005]	0.284	8.91	32.6	16.4	524	30.7	23.9	60.9	-	-	6090	65.4	1.15	1.18	2.17
Romania soils [Dumitru, M. et al, 2011]	0.43	13.0	-	26.7	175-1820	35.0	21.3	87	-	-	-	-	-	-	-
Romania (Maramures county) [Manea, A. et al, 2018]	0.75	11	23	20	554	22	57	78	-	-	-	-	-	-	-
Romania (Galati) [Pantelica, A. et al., 2013]	<2.5	13.1	84	-	538	67	-	106	-	-	2900	-	0.83	0.76	3.15
Reference values (land with sensitive use of soils) [Order no. 756/1997]	1 3 5	15 30 50	30 100 300	20 100 200	900 150 0 250 0	20 75 150	20 50 100	100 300 600	- 150 300	-	-	-	-	-	-
Normal															

Alert threshold Intervention threshold		

[1] average values in upper layer (aqua regia digestion); *[Cullen, J.T. and Maldonado, M.T., 2013].

Cadmium (Cd) in Soil

The average concentration of Cd in agricultural soils did not exceed the normal limits provided by [Order no. 756/1997] (see Table 5) and is below the average value reported at the European and national levels.

Tulucesti. The level of Cd in the upper layer of soil varies within the limits of 0.060±0.002 - 0.238±0.001 mg kg^{-1} d.w. (0-5 cm), and 0.051±0.001-0.262±0.007 mg kg^{-1} d.w. (5-30 cm). The lowest values were recorded in the sampling sites T-2, T-3, T-4, and T-5 in soils with a coarse texture (fine sand). The highest values are present in sampling sites T-1 and T-6 on textures ranging from coarse (medium sand) to medium (silty loam, medium loam and fine sandy loam). Overall, the average Cd concentration in the 0-5 cm layer is 0.130±0.002 mg kg^{-1} d.w., and in the 5-30 cm layer, 0.132±0.003 mg kg^{-1} d.w.

Sendreni. The average Cd content varies between 0.142±0.001 and 0.176±0.001 mg kg^{-1} d.w. (0-5 cm), and between 0.130±0.002 and 0.137±0.003 mg kg^{-1} d.w. (5-30 cm). Soil texture in coarse (fine sand) and medium (sandy silt). The average value of Cd concentration in the 0-5 cm layer is 0.159±0.002 mg kg^{-1} d.w., and in the 5-30 cm layer is 0.134±0.003 mg kg^{-1} d.w.

Vadeni. The average Cd level varies from 0.127±0.001 and 0.157±0.003 mg kg^{-1} d.w. (0-5 cm layer) to 0.108±0.001 and 0.155±0.001 mg kg^{-1} d.w.(5-30 cm layer). The soils have coarse (fine sand, medium sand) and medium (sandy dust) textures. Average Cd registers a value of 0.140±0.003 mg kg^{-1} d.w. (0-5 cm), and a value of 0.136±0.001 mg kg^{-1} d.w. (5-30 cm).

Cobalt (Co) in Soil

Tulucesti. The Co concentration is between 2.873±0.451 and 8.272±0.142 mg kg^{-1} d.w. (0-5 cm) and between 5.380±0.117 and 8.577±0.280 mg kg^{-1} d.w. (5-30 cm). The average value is 6.334±0.280 mg kg^{-1} d.w. for the 0-5 cm layer and 7.134±0.116 mg kg^{-1} d.w. for the 5-30 cm layer.

Sendreni. Co shows values of 8.798±0.0.072-8.833±0.141 mg kg^{-1} d.w. (0-5 cm), and of 8.811±0.162-9.467±0.163 mg kg^{-1} d.w. (5-30 cm). The average value on 0-5 cm is 8.816±0.107 mg kg^{-1} d.w., and on 5-30 cm, it is 9.139±0.1162 mg kg^{-1} d.w.

Vadeni. The Co content ranges between 5.289±0.123-11.190±0.225 mg kg^{-1} d.w. (0-5 cm), and between 4.876±0.123-10.060±0.225 mg kg^{-1} d.w.(5-30 cm). The highest values are recorded at the V-2 sampling site on the right side of the Sendreni-Baldovinesti road, where the soil is of medium texture (sandy silt). The average value is 7.775±0.178 mg kg^{-1} d.w. for the 0-5 cm layer and 6.884±0.185 mg kg^{-1} d.w. for the 5-30 cm layer.

Chromium (Cr) in Soil

Compared to the other metals investigated in this work, Cr shows the highest values, exceeding the normal limits (30 mg kg^{-1} d.w.).

Tulucesti. Cr varies within wide limits, from 83.270±0.518 mg kg^{-1} d.w. (5-30 cm, T-2b) to 383.100±5.378 mg kg^{-1} d.w. (0-5 cm, T-1a). Thus, **67% of the analyzed samples** (T-3, T-4, T-5, T-6) **exceed the alert threshold for sensitive uses, which represents a potentially significant pollution level, 17% are between the normal value and the alert threshold for sensitive uses** (T-2a), and **16% of the samples exceed the intervention threshold for sensitive uses** (T-1a), **which represents significant pollution**. At 0-5 cm, the concentration of Cr in agricultural soils is from 97.620±1.707 mg kg^{-1} d.w.to 383.100±5.378 mg kg^{-1} d.w., and at 5-30 cm, from 83.270±0.518 mg kg^{-1} d.w.to 175.500±

1.424 mg kg^{-1} d.w.. The average value is 158.253±2.696 mg kg^{-1} d.w. (0-5 cm) and 122.362±1.324 mg kg^{-1} d.w. (5-30cm).

Sendreni. The Cr concentration in the 0-5 cm and the 5-30 cm layer respectively, **exceeds the alert threshold for sensitive uses (potentially significant pollution)**. Thus, for the 0-5 cm depth, the Cr level is within the limits of 191.000±5.868-215.400±5.758 mg kg^{-1} d.w., and for the 5-30 cm depth, it is between 183.500±2.841-205.300±6.398 mg kg^{-1} d.w. The average value for the first 5 cm of soil is 203.200±5.813 mg kg^{-1} d.w., and for the next 25 cm, 194.400±4.620 mg kg^{-1} d.w.

Vadeni. The Cr content exceeds the alert threshold for sensitive uses (potentially significant pollution) for both soil depths. For the V-2b (5-30 cm) site, the Cr concentration exceeds the intervention threshold for sensitive uses (significant pollution), with a value of 349.600±5.840 mg kg^{-1} d.w. In the 0-5 cm layer, the values ranged between 117.100±1.039 to 277.400±6.144 mg kg^{-1} d.w., and in the 5-30 cm layer, between 123.400±2.345 to 349.600±5.840 mg kg^{-1} d.w. The average value for the first layer is 206.933±5.555 mg kg^{-1} d.w., and for the second, 230.200±3.985 mg kg^{-1} d.w.

Copper (Cu) in Soil

Tulucesti. The average content of Cu in the 0-5 cm layer is between 17.110±0.059 mg kg^{-1} d.w. and 61.082±0.539 mg kg^{-1} d.w. In the next 25 cm, Cu records values between 17.120±0.156 mg kg^{-1} d.w.and 68.151±0.198 mg kg^{-1} d.w. All the analyzed samples exceed the reference value of 20 mg kg^{-1} d.w. The average concentration for the first 5 cm of soil is 30.904±0.230 mg kg^{-1} d.w., and for the next 25 cm, 30.887±0.221 mg kg^{-1} d.w.

Sendreni. In all the collected soil samples copper exceeds the normal value, but it is below the alert threshold. Cu is in the range of 18.970±0.115-22.930±0.309 mg kg^{-1} d.w. (0-5 cm), and it varies between 18.990±0.235 and 19.850±0.323 mg kg^{-1} d.w. (5-30 cm). The average content for the 0-5 cm depth is 24.107±0.175 mg kg^{-1} d.w., and for the 5-30 cm depth, 22.520±0.175 mg kg^{-1} d.w.

Vadeni. In all the analyzed soil samples, cooper exceeds the normal value. Thus, in the 0-5 cm layer, the Cu concentration is 23,350±0,495-31,510±0,256 mg kg^{-1} d.w., while in the 5-30 cm layer, it registers values of 24,510±0,168-34,180±0,217 mg kg^{-1} d.w. The average value is 28.163±0.404 mg kg^{-1} d.w. (0-5 cm), and 27.923±0.219 mg kg^{-1} d.w. (5-30 cm).

Manganese (Mn) in Soil

Tulucesti. The concentration of Mn in all the collected soil samples falls within the normal range. The average content of Mn in the agricultural layers ranges between 177.045±3.869 and 317.845±7.061 mg kg^{-1} d.w., with an average of 241.612±4.994 mg kg^{-1} d.w., on 0-5 cm, and from 182.245±2.313 to 359.445±0.746 mg kg^{-1} d.w., with an average of 266.312±6.784 mg kg^{-1} d.w., on 5-30 cm.

Sendreni. The average concentration of Mn does not exceed the normal limit provided by the legislation in force and falls within the values reported in the literature (Table 5). In the agricultural soil of Sendreni, the Mn level is between 223.446±5.828-417.846±9.798 mg kg^{-1} d.w., with an average of 320.646±7.813 mg kg^{-1} d.w. (0-5 cm), and between 253.246±6.940 and 276.445±6.413 mg kg^{-1} d.w., with an average of 264.846±6.677 mg kg^{-1} d.w. (5-30 cm).

Vadeni. The assessed agricultural soils show average values of the Mn level similar to the territories of Tulucesti and Sendreni. The results obtained for this element are far below the normal value mentioned in the Romanian legislation. In the 0-5 cm layer, the Mn content varies from 176.146±2.548 to 256.646±11.610 mg kg^{-1} d.w., and an average value of 224.212±6.395 mg kg^{-1} d.w., while in the 5-30 cm layer, Mn has values situated between 153.845±2.848 and 297.745±4.852 mg kg^{-1} d.w., and an average value of 215.379±3.230 mg kg^{-1} d.w.

Nickel (Ni) in Soil

The content of Ni in all the assessed agricultural soils exceeds the normal values for all analyzed samples.

Tulucesti. The Ni content exceeds 1.7 to 2 times the normal content of 20 mg kg^{-1} d.w., but does not reach the alert threshold for sensitive uses. In the 0-5 cm layer, the concentration varies from

35.265±0.776 to 44.455±0.356 mg kg⁻¹ d.w., and in the 5-30 cm layer, from 34.881±0.113 to 41.665±0.369 mg kg⁻¹ d.w. The average values are 39.624±0.442 mg kg⁻¹ d.w. (0-5 cm) and 38.854±0.306 mg kg⁻¹ d.w. (5-30 cm).

Sendreni. The Ni content is similar to that recorded for agricultural soils from Tulucesti. The depth variation of Ni is as follows: for 0-5 cm, Ni is within the limits of 35.265±0.776-44.455±0.356 mg kg⁻¹ d.w., with an average of 39.153±0.430 mg kg⁻¹ d.w., and for 5-30 cm, is within the limits of 34.881±0.113-41.665±0.542 mg kg⁻¹ d.w., having an average of 37.073±0.334 mg kg⁻¹ d.w.

Vadeni. The concentration of Ni in the agricultural layer of Vadeni is slightly higher than in the other territories studied, exceeding 1.6-2.8 times the normal value, but does not reach the alert threshold for sensitive (agricultural) uses. The Ni content registers values of 31.338±0.094-46.197±0.416 mg kg⁻¹ d.w (0-5 cm layer), with an average of 40.488±0.565 mg kg⁻¹ d.w, and values of 30.157±0.633-55.656±0.167 mg kg⁻¹ d.w (5-30 cm layer), with an average of 42.887±0.624 mg kg⁻¹ d.w.

Zinc (Zn) in Soil

The average content of Zn in the investigated agricultural soils falls, on the whole, within normal limits, except in a few areas from Tulucesti and Vadeni, where the concentration exceeds the normal limit of 100 mg kg⁻¹ d.w. Concentrations exceeding this value are attributed to complex fertilizers and industrial emissions.

Tulucesti. Zn values fall between 30.395±1.751 and 136.586±1.229 mg kg⁻¹ d.w (0-5 cm) and are from 65.145±0.847 to 122.690±2.252 mg kg⁻¹ d.w (5-25 cm). The average is 87.013±1.178 mg kg⁻¹ d.w for 0-5 cm and 82.612±1.178 mg kg⁻¹ d.w for 5-25 cm.

Sendreni. The concentration of zinc ranked between 69.370±2.034 and 79.501±0.440 mg kg⁻¹ d.w (0-5 cm) and from 63.306±1.805 to 71.349±1.068 mg kg⁻¹ d.w (5-30 cm). The average is 74.435±1.237 mg kg⁻¹ d.w for 0-5 cm and 67.327±1.437 mg kg⁻¹ d.w for 5-25 cm.

Vadeni. The content of zinc is similar to the other two territories, recording values of 73.098±0.363-102.587±0.718 mg kg⁻¹ d.w., in the 0-5 cm layer, with an average of 89.141±0.945 mg kg⁻¹ d.w., and values of 73.457±0.850-103.886±0.325 mg kg⁻¹ d.w., with an average of 89.094±0.850 mg kg⁻¹ d.w., in the 5-30 cm layer.

Lead (Pb) in Soil

Analytical results show that the concentration of Pb in the agricultural soils of Tulucesti, Sendreni and Vadeni is within normal limits without significant variations.

Tulucesti. The level of Pb is within the limits of 3.207±0.128-12.760±0.834 mg kg⁻¹ d.w., with an average of 6.429±0.455 mg kg⁻¹ d.w. (0-5 cm), and between 3.902±0.382 - 19.940±1.314 mg kg⁻¹ d.w., with an average of 7.991±0.543 mg kg⁻¹ d.w. (5-30 cm).

Sendreni. Lead registers values of 13.630±0.329-15.070±0.255 mg kg⁻¹ d.w., with an average of 14.350±0.292 mg kg⁻¹ d.w., in the 0-5 cm layer, and values of 13.310±0.462 - 14.760±0.503 mg kg⁻¹ d.w., with an average of 14.035±0.482 mg kg⁻¹ d.w., in the 5-30 cm layer.

Vadeni. The average Pb content is within the limits of 10.370±0.767-14.250±0.354 mg/kg s.u., with an average of 11.980±0.507 mg/kg s.u., in the 0-5 cm layer, and 6.308±0.432-13.310±0.653 mg/kg s.u., with an average of 9.796±0.437 mg/kg s.u., in the 5-30 cm layer.

Other Major and Trace Elements in Soil

In conducting soil analysis within the Lower Danube Basin, PIGE nuclear method proved particularly useful in identifying and quantifying light elements, including Al, Na, Mg, Si, Cl, and F. Some of these elements, such as fluorine, can be hazardous even in low amounts. Figure 5 illustrates the distribution of light elements in the upper layer of the agricultural soil in the Lower Danube Basin.
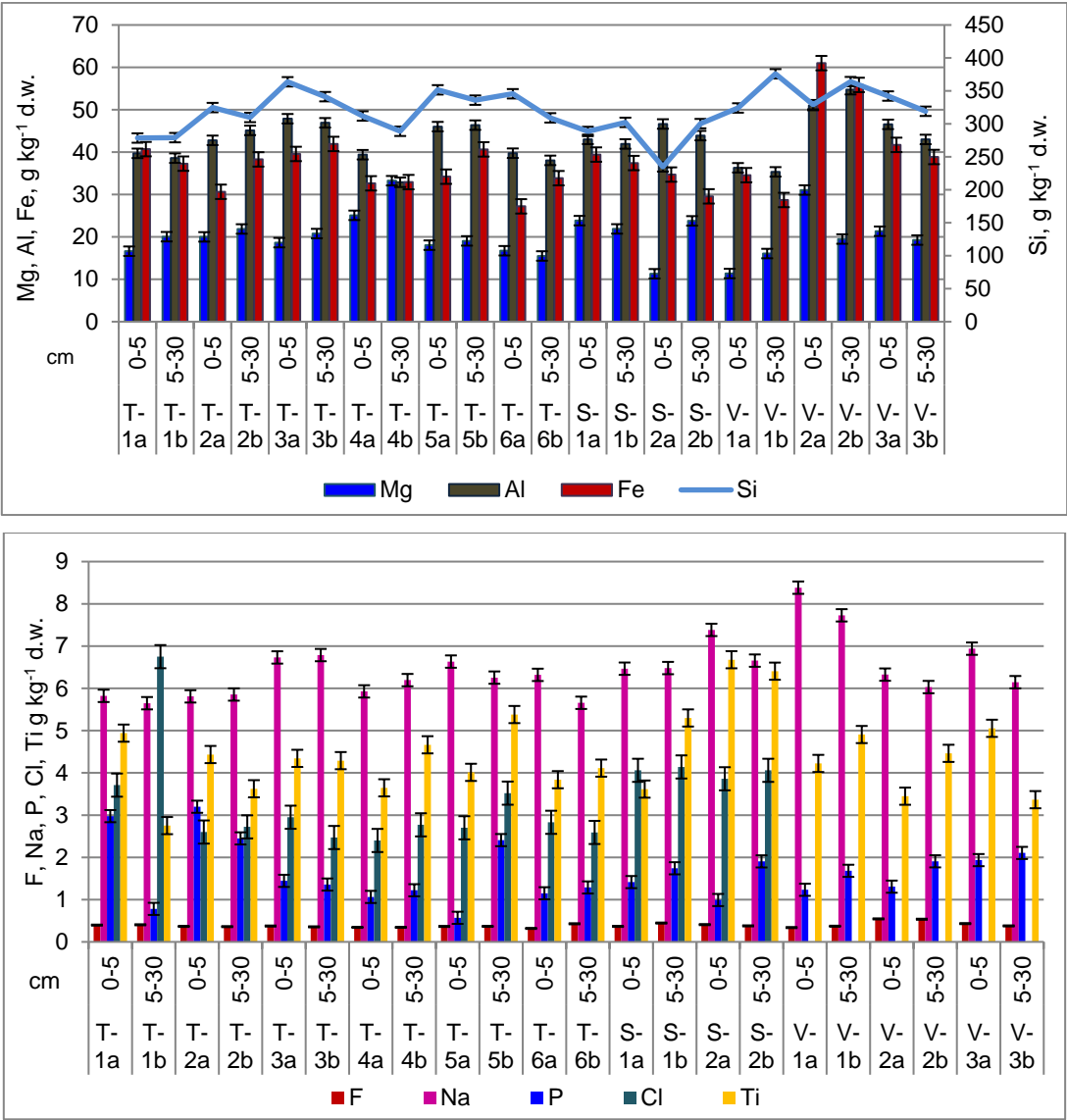
Figure 5. Light elements distribution and concentration in upper layers of agicultural soils in the Lower Danube Basin.

In the *Tulucesti* region, sodium levels in the 0-5 cm layer range from 5.810±0.080 to 6.731±0.105 g kg^{-1} d.w., while in the 5-30 cm layer vary between 5.648±0.198 and 6.787±0.110 g kg^{-1} d.w. Aluminum content ranges between 39.726±0.795 and 47.889±0.627 g kg^{-1} d.w. (0-5 cm) and 32.886±0.474-46.374 g kg^{-1} d.w. (5-30 cm). Silicon concentration in the 0-5 cm section is between 278.561±27.299 and 363.827±19.787 g kg^{-1} d.w., and in the 5-30 cm layer, it ranges from 279.181±22.614 to 341.306±21.874 g kg^{-1} d.w. Chlorine shows the lowest values compared to other elements; in the 0-5 cm layer, it fall within the range of <2,400-<3,710 g kg^{-1} d.w., while in the 5-30 cm layer it varies between <0,2470-<6,750 g kg^{-1} d.w.

In the *Sendreni* area, the uppermost soil layer (0-5 cm) has a sodium content ranging from 6.465±0.153 to 7.383±0.177 g kg^{-1} d.w. In the underlying layer (5-30 cm), the concentration of sodium ranges between 6.480±0.156 and 6.656±0.153 g kg^{-1} d.w. The aluminum level ranges from 43.019±0.860 to 46.649±0.840 g kg^{-1} d.w. (0-5 cm) and from 41.929±1.090 to 43.901±1.010 g kg^{-1} d.w. (5-30 cm). Silicon content follows a similar trend, with concentrations ranging from 234.834±25.832 to 288.548±25.681 g kg^{-1} d.w. in the first 5 cm of soil and from 300.419±23.433 to 302.290±27.206 g kg^{-1} d.w. in the next 25 cm. Chlorine, on the other hand, has low concentrations that fall below <3.860-<4.060 g kg^{-1} d.w. at 0-5 cm and <4.060-<4.140 g kg^{-1} d.w. at 5-30 cm.

In the *Vadeni* land, in the top 5 cm of soil, the sodium content ranges from 6.325±0.164 to 8.382±0.184 g kg⁻¹ d.w., while in the 5-30 cm layer, it is between 6.030±0.217 to 7.728±0.162 g kg⁻¹ d.w. In the 0-5 cm layer, aluminum concentrations range from 36.316±0.654 to 51.013±1.122 g kg⁻¹ d.w., and in the 5-30 cm layer, they range from 35.351±0.742 to 54.737±0.985 g kg⁻¹ d.w. The silicon content in the top 5 cm of soil is comparable to that of agricultural soil found in the Tuluceşti and Sendreni regions. The values range from 324.148±34.036 to 342.263±32.515 g kg⁻¹ d.w. In the 5-30 cm layer, the silicon content ranges from 319.154±27.447 to 375.991±24.439 g kg⁻¹ d.w.

The analysis of agricultural soils has shown a variable accumulation of Fe between soil layers and territorial distribution. In *Tulucesti*, higher concentrations of Fe were observed at the depth of 5-30 cm, with values ranging from 32.935±3.635-41.937±3.359 g kg⁻¹ d.w. compared to the 0-5 cm layer, where the values vary between 27.219±3.004 and 39.579 ±3.260 g kg⁻¹ d.w. However, soil sampled from the site T-1 shows higher values in the 0-5 cm layer (40.719±4.316 g kg⁻¹ d.w.) compared to the underlying 5-30 cm layer (37.289±7.048 g kg⁻¹ d.w.). In *Sendreni* and *Vadeni*, higher concentrations of Fe were found in the upper 0-5 cm layer, with values ranging from 34.718±4.826 g kg⁻¹ d.w. to 39.432±4.968 g kg⁻¹ d.w. and from 34.576±3.734 g kg⁻¹ d.w. to 61.005±4.758 g kg⁻¹ d.w.   respectively. In the 5-30 cm layer, the concentrations vary between 29.574±4.820 g kg⁻¹ d.w. and 37.432± 4.529 g kg⁻¹ d.w. in Sendreni and between 28.717±3.848 and 38.861±5.596 g kg⁻¹ d.w. in *Vadeni*. According to [Kabata-Pendias, A., 2011], the average value of Fe in soil is 35 g kg⁻¹. The highest value of Fe concentration was recorded at sampling site V-2, at both depths, with values of 61.005±4.758 g kg⁻¹ d.w. and 55.863±4.637 g kg⁻¹ d.w.

Titanium values are lower than the average concentration in soil presented in Table 5. In *Tulucesti*, the values range between 3.646±0.600 g kg⁻¹ d.w. and 4.940±1.279 g kg⁻¹ d.w. in the 0-5 cm layer and between 2.752±1.016 g kg⁻¹ d.w. and 5.380±0.727 g kg⁻¹ d.w. in the 5-30 cm layer. In *Sendreni*, the concentration of Ti in the 0-5 cm layer ranges between 3.616±0.1.074-6.677±1.489 g kg⁻¹ d.w., and in the 5-30 cm layer, the values are between 5.299±1.160 and 6.406±1.006 g kg⁻¹ d.w. In *Vadeni*, the values vary between 3.448±0.952 g kg⁻¹ d.w. and 5.054±1.228 g kg⁻¹ d.w. in the 0-5 cm layer and between 3.365±0.905 and 4.907±9.981 g kg⁻¹ d.w. in the 5-30 cm layer.

Through PIGE technique, it was possible to identify fluorine, an extremely harmful element that negatively impacts ecosystems. Fluorine is typically associated with bone disease [https://www.cancercenter.com/risk-factors/fluoride] and can disrupt the processes of photosynthesis and respiration in plants [Kumar, K. et al., 2017]. In most living organisms, the concentration of fluoride is less than 10 μg/g d.w. [Bhat, N. et al., 2015]. According to [Kabata-Pendias, A., 2011], soils worldwide have an average fluoride content of 321 mg kg⁻¹, while the continental crust has a value of 625 mg kg⁻¹. In **the analyzed soils fluoride exceeds the global average**. For instance, in *Tulucesti*, fluoride values range from 0.319±0.010 to 0.397±0.038 g kg⁻¹ d.w. in the 0-5 cm layer and from 0.345±0.014 to 0.429±0.016 g kg⁻¹ d.w. in the 5-30 cm layer. In *Sendreni*, the values vary between 0.367±0.0.28-0.379±0.031 g kg-1 d.w. in the 0-5 cm depth and between 0.379±0.031 and 0.446±0.033 g kg⁻¹ d.w. in the 5-30 cm section. The fluoride concentration in the 0-5 cm layer on the *Vadeni* territory is 0.339±0.016-0.544±0.029 g kg⁻¹ d.w., while in the 5-30 cm layer it is 0.371±0.030-0.536±0.031 g kg⁻¹ d.w. Notably, sampling point V-2, located on the right side of the European road E87 in the Sendreni-Baldovinesti segment, has slightly higher fluoride concentrations at both depths compared to other sampling points on the territory of Vadeni. The main sources of soil contamination with fluoride are emissions from metallurgical activities and the use of phosphate fertilizers and pesticides [WHO, 2019].

3.3. Mineralogical and Microstructural Analysis of Soil

Soils encompass a complex array of chemical components, comprising both mineral factions such as clays, oxides, and quartz as well as organic fractions constituted by organic matter in various stages of decomposition. Additionally, soils contain water and air. The intricate composition of soils renders them a challenging material to study, requiring a comprehensive approach that considers the interplay of the various components.

Based on the ATR-FTIR spectra featured in Figure 6, it is evident that the absorption bands of the analyzed soil samples share similarities, but their peak intensities differ. This indicates the presence of various functional groups of chemical elements, which are characteristic of both clay minerals and non-clay minerals.
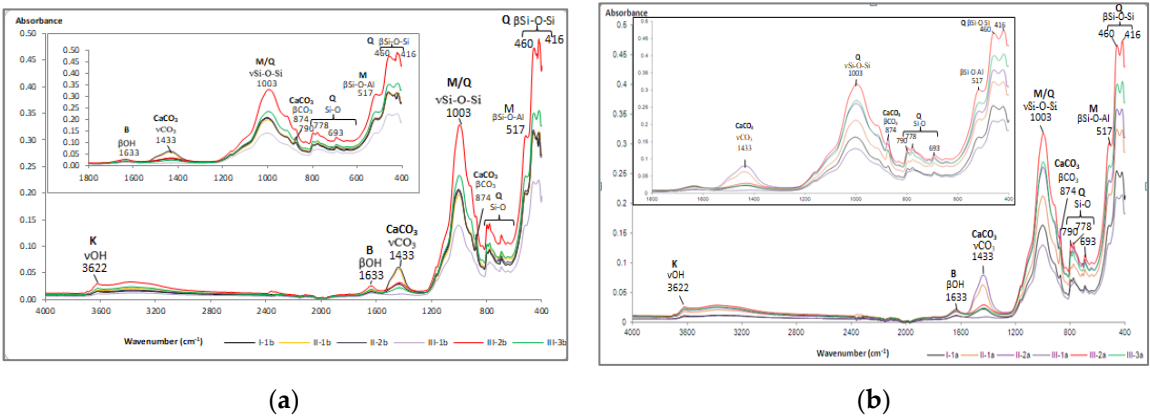

(a)   (b)

Figure 6. Soil ATR-FTIR spectra in the 4000-400 cm^{-1} region, and 1800-400 cm^{-1}: (**a**) 0-5 cm layer; (**b**) 5-30 cm layer.

Within the spectral range of 1500-400 cm^{-1}, known as the "spectral fingerprint domain" [Bulgariu, D. et al, 2018], distinctive absorption bands of clay minerals including montmorillonite $((Na,Ca)_{0.33}(Al,Mg)_2(Si_4O_{10})(OH)_2 \cdot nH_2O)$ and kaolinite $(Al_2Si_2O_5(OH)_4))$ have been identified. Additionally, non-clay minerals such as quartz (SiO_2), feldspars (orthose $(KAlSi_3O_8)$, albite $(NaAlSi_3O_8))$, and calcite $(CaCO_3)$ have also been recognized. Table 6 displays the ATR-FTIR peaks that represent the functional groups associated with the primary minerals present in the studied soils. To emphasize the absorption bands in the 850-1250 cm^{-1} range, the ATR-FTIR spectra were deconvoluted, as illustrated in Figure 7 [Moraru, S.S. et al, 2019].

Table 6. Characteristic absorption bands associated with the vibrations of the functional groups of the main minerals found in the selected soil samples [Arbanas (Moraru) S.-S. 2022].

Mineral type	Absorption band (cm^{-1})	Band assignment[1]	Reference
		Clay minerals	
Montmorillonite	830	*β(Al-OH-Mg)*	840-830 cm^{-1} β(Al-OH-Mg) [Volkov, D.S. et al, 2021]
	912	*β(Al-Al-OH)*	930-910 cm^{-1} β(OH) [Volkov, D.S. et al, 2021]
			915 cm^{-1} β(OH) [Stoica, E. et al, 1986]
			916 cm^{-1} β(OH) [Madejova, J. și Komadel, P., 2001]
	1633	*β(OH)*	1635 cm^{-1} β(OH) [Müller, C.M. et al, 2014]
	3390	*ν(OH)*	3392 cm^{-1} [Gosav, S. et al, 2019]
	3620	*inner surface ν(OH)*	3700-3600 cm^{-1} inner surface ν(OH) [Müller, C.M. et al, 2014]
			3610-3621 cm^{-1} abnormal montmorillonite [Crăciun, C., 1987]
			3620 cm^{-1} ν(OH) [Volkov, D.S. et al, 2021]
			3627 cm^{-1} [Gosav, S. et al, 2019]
Kaolinite	419	*β(Si-O-Si)*	430-420 cm^{-1} β(Si-O) [Volkov, D.S. et al, 2021]
	912	*β(Al-OH-Al)*	930-910 cm^{-1} (β(OH) [Volkov, D.S. et al, 2021]

Mineral type	Absorption band (cm⁻¹)	Band assignment[1]	Reference
	1032	$\nu_{as}(Si\text{-}O\text{-}Si)$	915 cm⁻¹ (β(OH) [Stoica, E. et al, 1986], [Müller, C.M. et al, 2014], [Madejova, J. and Komadel, P., 2001]
			1034 cm⁻¹ [Gosav, S. et al, 2019]
			1037 cm⁻¹ ν$_{as}$(Al-O) [Volkov, D.S. et al, 2021]
			1038 cm⁻¹ ν$_{as}$(Si-O-Si) [Stoica, E. et al, 1986]
	3620	$inner\ \nu(OH)$	3620 cm⁻¹ ν(OH) [Volkov, D.S. et al, 2021], [Stoica, E. et al, 1986], [Müller, C.M. et al, 2014], [Madejova, J. and Komadel, P., 2001]
	3695	$inner\text{-}surface$ $\nu(OH)$	3690-3680 cm⁻¹ ν(Si-OH) [Volkov, D.S. et al, 2021]
			3694 cm⁻¹ inner-surface ν(OH) [Madejova, J. and Komadel, P., 2001]
			3695 cm⁻¹ (ν(OH)) [Stoica, E. et al, 1986], [Müller, C.M. et al, 2014]
Non-clay minerals			
Quartz	457	$\beta(Si\text{-}O\text{-}Si)$	450 cm⁻¹ β(O-Si-O) [Volkov, D.S. et al, 2021]
			452 cm⁻¹ [Gosav, S. et al, 2019]
	517	$\beta(O\text{-}Si\text{-}O)$	517-513 cm⁻¹ β(O-Si-O) [Volkov, D.S. et al, 2021]
			512 cm⁻¹ SiO₂ [Stoica, E. et al, 1986]
	692	$\beta(Si\text{-}O\text{-}Si)$	697-696 cm⁻¹ β(Si-O-Si) [Volkov, D.S. et al, 2021]
			693 cm⁻¹ SiO₂ [Stoica, E. et al, 1986]
	778	$\nu(Si\text{-}O)$	774 cm⁻¹ α-SiO₂, Si-O-Si [Volkov, D.S. et al, 2021]
			778 cm⁻¹ SiO₂ [Stoica, E. et al, 1986]
			779 cm⁻¹ ν(Si-O) [Madejova, J. and Komadel, P., 2001]
	796	$\nu_{sim}(Si\text{-}O\text{-}Si)$	796 cm⁻¹ ν$_{sim}$(Si-O-Si) [Volkov, D.S. et al, 2021]
			797 cm⁻¹ ν(Si-O) [Madejova, J. and Komadel, P., 2001]
			798 cm⁻¹ SiO₂ [Stoica, E. et al, 1986]
	1001	$\nu(Si\text{-}O)$	1010-995 cm⁻¹ ν(Si-O) [Volkov, D.S. et al, 2021]
			1100-950 cm⁻¹ ν(Si-O) [Palacio, S. et al, 2014]
	1111	$\nu_{as}(Si\text{-}O\text{-}Si)$	1115-1105 cm⁻¹ amorphous silica [Volkov, D.S. et al, 2021]
	1168	$\nu_{as}(Si\text{-}O\text{-}Si)$	1165-1153 cm⁻¹ specific SiO₂ structure [Volkov, D.S. et al, 2021]
			1166 cm⁻¹ SiO2 - cristobalite [Stoica, E. et al, 1986]
Orthoclase and albite	646	$\beta(O\text{-}Si(Al)\text{-}O)$	645-640 cm⁻¹ β(Si-O) [Volkov, D.S. et al, 2021]
	989	$\nu(Si\text{-}O)$	1200-900 cm⁻¹ [Müller, C.M. et al, 2014]
Calcite	712	$\beta(C\text{-}O)$	713-710 cm⁻¹ CaCO₃ [Bulgariu, D. et al, 2018]
			712 cm⁻¹ CaCO₃ [Stoica, E. et al, 1986]
			715 cm⁻¹ β(C-O) in plane [Palacio, S. et al, 2014]
	874	$\beta(C\text{-}O)$	881-873 cm⁻¹ CaCO₃ [Bulgariu, D. et al, 2018]
			874 cm⁻¹ β(C-O) in plane [Palacio, S. et al, 2014]

Mineral type	Absorption band (cm^{-1})	Band assignment[1]	Reference
Dolomite	1433	$\nu_{as}(C\text{-}O)$	875 cm^{-1} CaCO$_3$ [Volkov, D.S. et al, 2021], [Müller, C.M. et al, 2014] 877 cm^{-1} CaCO$_3$ [Stoica, E. et al, 1986] 1400 cm^{-1} $\nu_{as}(C\text{-}O)$ [Müller, C.M. et al, 2014] 1410-1435 cm^{-1} CaCO$_3$ [Bulgariu, D. et al, 2018] 1435 cm^{-1} CaCO$_3$ [Stoica, E. et al, 1986] 1450-1410 cm^{-1} $\nu_{as}(C\text{-}O)$ [Palacio, S. et al, 2014]
	1433	$\nu_{as}(C\text{-}O)$	1450-1430 cm^{-1} CaMg(CO$_3$)$_2$ [Bulgariu, D. et al, 2018] 1432 cm^{-1} CaMg(CO$_3$)$_2$ [Stoica, E. et al, 1986] 1433 cm^{-1} $\nu_{as}(CO_3^{2-})$ [Mroczkowska-Szerszeń, M. and Orzechowski, M., 2018]
Gypsum	646	$\beta(S\text{-}O)$	645-640 cm^{-1} $\beta(S\text{-}O)$ [Volkov, D.S. et al, 2021] 680-610 cm^{-1} $\beta(S\text{-}O)$ [Palacio, S. et al, 2014]
	1111	$\nu(S\text{-}O)$	1140-1080 cm^{-1} $\nu(S\text{-}O)$ [Palacio, S. et al, 2014] 1111 cm^{-1} CaSO$_4 \cdot$ 2 H$_2$O [Stoica, E. et al, 1986]

[1] ν-stretching vibration, $\nu_{as/sim}$-asymmetric/ symmetric stretching vibration, β- bending vibration .
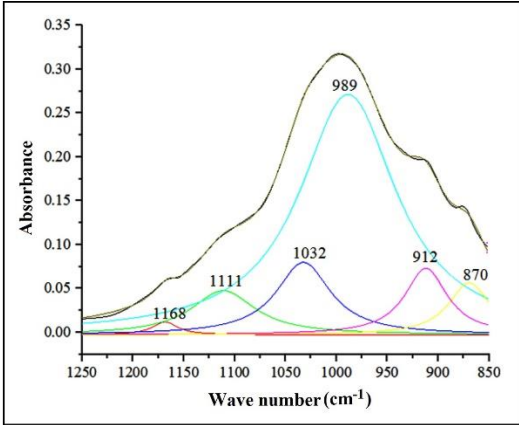

Figure 7. Deconvolution of the IR absorption bands in the range 1250-850 cm^{-1}.

The selected soil samples were found to contain montmorillonite and kaolinite minerals from the category of clay minerals. The stretching vibrations of the hydroxyl functional group (-OH) were attributed to these domains within the limits of 3390-3620 cm^{-1} and 3620-3695 cm^{-1}, respectively. [Craciun, C., 1987] mentioned that the values of wavenumbers in the range 3610-3621 cm^{-1} are characteristic of abnormal montmorillonite, a category of mineral widespread in most soils, which presents a single dehydroxylation reaction, while [Stoica, E. et al, 1986] reported that in the case of abnormal montmorillonite, the stretching vibration of the -OH group is highlighted by the peak with the value 3625 cm^{-1}.

In the case of kaolinite, the asymmetric stretching vibration of the Si-O-Si group in the 1032 cm^{-1} area was noticeable. The bending vibrations attributed to functional groups Al-OH-Al (912 cm^{-1}), Al-OH-Mg (830 cm^{-1}), and Si-O-Si (419 cm^{-1}) were recorded in the 1000-400 cm^{-1} area from the structure of clay minerals.

The peaks at 778 cm^{-1}, 796 cm^{-1}, 1001 cm^{-1}, 1111 cm^{-1}, and 1168 cm^{-1} are attributed to the symmetric and asymmetric stretching vibrations of the Si-O and Si-O-Si groups in the quartz structure. The highest absorbance was recorded for the peak at wave number 1001 cm^{-1}. [Volkov, D.S. et al., 2021] assigned the bands in the range 1115-1105 cm^{-1} (1001 cm^{-1} and 1111 cm^{-1} for the selected soils) to the asymmetric stretching vibration of the Si-O-Si group in amorphous silica. At the same time, the

deformation vibrations of the Si-O-Si group, fully registered in the range 692-457 cm^{-1}, are noted. [Stoica, E. et al, 1986] assigned the 1166 cm^{-1} peak to cristobalite, a variety of quartz with a tetragonal crystal structure, and [Volkov, D.S., et al, 2021] reported that the wave number 778 cm^{-1} corresponds to α-quartz, variety with the trigonal crystalline structure.

A particular situation is given by the absorption band of 1111 cm^{-1}, highlighted in the deconvolution zone of the complex of bands in the range 1250-850 cm^{-1} (Figure 7), which, according to [Stoica, E. et al, 1986], is associated with gypsum (CaSO$_4 \cdot$ 2 H$_2$O). The vibrational mode of the SO$_4^{2-}$ ion in the 1111 cm^{-1} band corresponds to the deformation vibration associated with the 646 cm^{-1} peak, reduced in intensity. Close values for sulfate vibrational modes are reported by [Al Dabbas, M. et al. a., 2014], [Volkov, D.S., et al, 2021], and [Palacio, S. et al. a., 2014].

The absorption band at 989 cm^{-1}, which is attributed to the Si-O group's stretching vibration, confirmed the presence of feldspars in the assessed soils. This absorption is highlighted by a pronounced peak in the deconvolution zone (Figure 7). Additionally, a secondary absorption band at 646 cm^{-1} was attributed to the O-Si(Al)-O group's deformation vibration, marked by a peak with low intensity (Figure 6). As stated by [Müller et al., 2014], calcite is characterized by two intense bands - 1400 cm^{-1}, attributed to the asymmetric stretching vibration, and 875 cm^{-1}, specific to the out-of-plane deformation vibration. The selected soil samples' absorption band values are around those replicated in the literature (Table 6). The values include a more intense absorption band, centered around 1433 cm^{-1}, attributed to the C-O group's asymmetric stretching vibration, and two narrower bands centered at 874 cm^{-1} and 712 cm^{-1}, characteristic of the same group's deformation vibration.

The ATR-FTIR spectra of the studied soil samples also highlights the presence of dolomite through the maximum peak centered at 1433 cm^{-1}, attributed to the asymmetric stretching vibration of the CO$_3^{2-}$ ion [Mroczkowska-Szerszeń, M. and Orzechowski, M., 2018], present in the chemical composition of this mineral (Ca Mg(CO$_3$)$_2$).

The intensity of the peaks associated with the characteristic absorption bands of calcite at 1433 cm^{-1} and 874 cm^{-1} (Figure 6) is directly proportional to the percentage of CaCO$_3$ in the soil.

The very low organic carbon percentages correlate with the absence of peaks in the ATR-FTIR spectrum. Specifically, the peaks at 2920-2926 cm^{-1} and 2850-2852 cm^{-1}, which are indicative of the symmetric and antisymmetric stretching vibrations of the functional group CH$_2$ [Gosav, S. et al., 2019], [Palacio, S. et al., 2014], are absent. The ATR-FTIR spectra of the soils examined in this study closely resemble those obtained by [Sion A. et al., 2020] for soils collected from parks located in the city of Galați, confirming the mineralogical footprint of the region.

The SEM-EDX technique was very valuable for examining the mineralogy of the soil and providing a semi-quantitative analysis of its elemental composition (Figure A1, Appendix A). Additionally, the results from SEM-EDX mapping (Figure A1, Appendix A) confirmed the findings obtained through the ATR-FTIR method. The analysis indicates a consistent elemental composition across the studied soils in the Lower Danube Basin.

The EDX spectra (Figure A1, Appendix A) revealed a predominant distribution of elements in the following order: O>Si>C>Al>Fe>Ca>K>N>Mg>Zn>Co>Ni>Ti>Na>Mn>P >Cr>S>Cl>Ga>Gd, for the 0-5 cm depth, and O>Si>C>Al>Fe>Ca>K>Mg>Gd>Ga>Ni>Co> Zn>Ti>Mn>Na>P>S>N>Cr>Cl, for the 5-30 cm depth (Tulucesti); O>Si>C>Al>Ca>Fe> Hg>K>Gd>Mg>Ga>Cu>Zn>Ni>Co>Na>Ti>Mn>Cr>P>S (0-5 cm) and O>Si>C>Al>Ca> Fe>K>Mg>Ga>Zn>Gd>Cu>Co>Ti>Mn>Ni>Na>V>Cr>P>S (5-30 cm) (Sendreni); similarly, in Vadeni, the vertical distribution of elements followed a comparable pattern: O> Si> C>Al> Fe> K> Ca> Gd> Ga> Zn> Mg> Cu> Co>Mn> Ti> Ni> Cr>Na> P> S (0-5 cm) and O>Si> C>Al> Fe>K>Ca> Co>Mg>Ti>N>Na>P>S (5-30 cm).

Out of the 24 identified elements, O and Si exhibited the highest concentration (Appendix A, Table A1). Notably, the O content in the investigated soils is slightly lower compared to the average value reported for the Earth's crust (46%) [https://ptable.com /#Properties/Series].

Silicon, a trace element present in plants and soils, exhibits variable concentrations across different soils and plant species. It constitutes 65.4% (SiO2) of the upper layer of European soils [Salminen, R., 2005] and accounts for 27% of the Earth's crust [https://ptable.com/#Properties/Series].

Silicon plays a crucial role in promoting plant growth and influencing the availability and accumulation of both macro- and micronutrients [Greger, M. et al., 2018]. In soil, silicon exists in both liquid and solid states, with the solid form being either amorphous (derived from the parent rock or living organisms) or crystalline (present in primary and secondary silicates and silicate materials) [Tubana, B.S. et al., 2016]. The presence of silicon in soil samples is validated using the ATR-FTIR method, which identifies the absorption bands characteristic of the chemical bonds formed by silicon with other elements in the soil's clay and non-clay minerals.

In the analyzed samples, varying concentrations of alkaline elements (sodium, magnesium, potassium, and calcium) were found (Appendix A, Table A1). The alkaline metals content in the Earth's crust, is in the order: Ca(5.0%) > Mg(2.9%) > Na(2.3%) > K(1.5%) [https://ptable.com/#Properti].

3.4. Assessment of Soil Contamination

The evaluation of soil contamination levels involved the use of pollution indices that facilitate comparisons between the degree of assessed soil contamination and the natural background incidence of identified metals.

The *Igeo* was estimated using the normal values specified in Romanian Order no. 756/1997 (Table 5) as the geochemical background [Arbanas (Moraru) S.-S. 2022]. The results obtained for *Igeo* are presented in Table 7.

According to the values obtained for *Igeo*, all the soil samples were considered to be in Class 0 - unpolluted with Cd, Co, Pb, Zn, and Cu (except the sampling sites T-1a, T-1b, V-3a), in Class 1 - unpolluted to moderate pollution with Ni (all the samples), Cr (sites T-2b), and Cu (sites T-1a, T-1b, V-2b, V-3a), Class 2 - moderate polluted with Cr (sites T-1a, S-1a, S-1b, S-2a, S-2b, V-2a, V-2b), Class 3 - moderate to high polluted with Cr (sites T-1a, S-1a, S-1b, S-2a, S-2b, V-2a, V-2b, V-3a, V-3b).

Table 7. Igeo index values calculated for the agricultural layers of soil in the Lower Danube Basin.

Sample site	Depth (cm)	$Igeo_{Cd}$	$Igeo_{Co}$	$Igeo_{Cr}$	$Igeo_{Cu}$	$Igeo_{Ni}$	$Igeo_{Pb}$	$Igeo_{Zn}$
T-1a	0-5	-2.67	-2.97	3.09	0.55	0.31	-1.23	-0.14
T-1b	5-30	-2.73	-1.62	1.73	0.33	0.36	-0.59	-0.29
T-2a	0-5	-3.89	-1.96	1.12	-0.26	0.49	-3.16	-0.52
T-2b	5-30	-3.74	-2.05	0.89	-0.26	0.26	-2.34	-0.61
T-3a	0-5	-4.65	-1.44	1.20	-0.53	0.57	-2.61	-1.04
T-3b	5-30	-4.88	-1.47	1.23	-0.63	0.47	-2.61	-1.20
T-4a	0-5	-4.15	-2.08	1.26	-0.81	0.23	-3.23	-1.31
T-4b	5-30	-4.04	-2.06	1.31	-0.75	0.29	-2.94	-1.17
T-5a	0-5	-4.63	-1.58	1.18	-0.78	0.42	-2.47	-1.11
T-5b	5-30	-4.85	-1.50	1.29	-0.81	0.22	-2.14	-1.16
T-6a	0-5	-2.66	-1.46	1.79	1.03	0.25	-1.75	-0.94
T-6b	5-30	-2.52	-1.39	1.96	1.18	0.22	-2.21	-0.98
S-1a	0-5	-3.09	-1.35	2.09	-0.66	0.47	-0.99	-1.11
S-1b	5-30	-3.46	-1.35	2.03	-0.66	0.47	-1.02	-1.24
S-2a	0-5	-3.40	-1.35	2.26	-0.39	0.24	-1.14	-0.92
S-2b	5-30	-3.52	-1.25	2.19	-0.60	0.27	-1.17	-1.07
V-1a	0-5	-3.25	-2.09	1.38	-0.36	0.06	-1.41	-1.04
V-1b	5-30	-3.27	-2.21	1.46	-0.29	0.01	-1.62	-1.03
V-2a	0-5	-3.47	-1.01	2.62	-0.02	0.62	-1.07	-0.71
V-2b	5-30	-3.36	-1.16	2.96	0.19	0.89	-1.17	-0.53
V-3a	0-5	-3.57	-1.72	2.33	0.07	0.55	-1.53	-0.55
V-3b	5-30	-3.79	-1.98	2.27	-0.26	0.51	-2.25	-0.74

$Igeo_i$	Class 0 $Igeo_i \leq 0$	Class 1 $0 < Igeo_i < 1$	Class 2 $1 < Igeo_i < 2$	Class 3 $2 < Igeo_i < 3$	Class 4 $3 < Igeo_i < 4$	Class 5 $4 < Igeo_i < 5$	Class 6 $Igeo_i > 5$

To evaluate the impact of anthropogenic activities, the Enrichment Factor (EF_i) was computed utilizing Aluminum (Al) as a normalizer element, which is found in abundant quantities in the geological background [Arbanas (Moraru) S.-S. 2022]. Considering the [Salminen, R. et al, 2005] values for Al in European topsoil, EF indicate Cd, Co, Pb (except site T-1b), Zn (sites T-3a, T-3b, T-5a, T-5b, T-6a, T-6b, S-1a, S-1b, S-2a, S-2b,) deficiency to minimal enrichment (Class 1), Cu (except sites T-1b, T-6b), Ni (sites T-1a, T-1b, T-2b, T-5b, T-6a, T-6b, S-1b, V-1a, V-2a, V-2b, V-3a, V-3b), Zn (sites T-a1, T-1b, T-2a, T-2b, T-4a, T-4b, V-1a, V-1b, V-2a, V-2b, V-3a) moderately enrichment (Class 2), Cr (except site T-1a, V-2a, V-2b, V-3a, V-3b), Cu (sites T-1a, T-6b), Ni (sites T-2a, T-3a, T-3b, T-4a, T-4b, T-5a, S-1b, V-1a, V-2a, V-2b) significant enrichment (Class 3), Cr (site T-1a, V-2a, V-2b) high enrichment (Class 4). Based on EF_i quantification, Table 8 displays the distribution of soil metal enrichment due to human activity.

Upon analyzing the EF values derived from the concentration of Cr, Cu, Ni, and Zn found in the uppermost layers of agricultural soils, it becomes apparent that the origins of these elements are multifaceted, encompassing both past and present factors. The extended duration of land cultivation and the industrial practices of the adjacent iron and steel plant are the primary contributors.

Table 8. ER_i index quantification for the agricultural layers of soil in the Lower Danube Basin.

Sample site	Depth (cm)	EF_{Cd}	EF_{Co}	EF_{Cr}	EF_{Cu}	EF_{Ni}	EF_{Pb}	EF_{Zn}
T-1a	0-5	0.60	0.49	32.46	5.59	4.73	1.62	3.47
T-1b	5-30	0.53	1.15	11.66	4.43	4.51	2.34	2.88
T-2a	0-5	0.26	0.98	8.24	3.17	5.34	0.43	2.65
T-2b	5-30	0.30	0.95	7.30	3.30	4.72	0.78	2.58
T-3a	0-5	0.16	1.44	8.99	2.71	5.80	0.64	1.90
T-3b	5-30	0.15	1.63	10.56	2.92	6.27	0.74	1.96
T-4a	0-5	0.29	1.21	12.24	2.92	6.01	0.55	2.06
T-4b	5-30	0.31	1.24	12.83	3.08	6.33	0.67	2.31
T-5a	0-5	0.16	1.37	9.26	2.38	5.47	0.74	1.89
T-5b	5-30	0.15	1.50	10.39	2.43	4.96	0.96	1.90
T-6a	0-5	0.37	0.85	8.04	4.73	2.76	0.69	1.21
T-6b	5-30	0.44	0.96	9.83	5.72	2.93	0.54	1.28
S-1a	0-5	0.42	1.40	15.12	2.25	4.94	1.79	1.65
S-1b	5-30	0.34	1.46	15.24	2.37	5.16	1.84	1.58
S-2a	0-5	0.36	1.47	17.95	2.87	4.44	1.70	1.99
S-2b	5-30	0.32	1.53	16.56	2.40	4.38	1.61	1.73
V-1a	0-5	0.50	1.13	12.51	3.74	5.02	1.81	2.34
V-1b	5-30	0.48	1.01	12.81	3.82	4.70	1.52	2.29
V-2a	0-5	0.31	1.71	21.24	3.40	5.31	1.64	2.11
V-2b	5-30	0.29	1.35	23.44	3.44	5.60	1.34	2.09
V-3a	0-5	0.25	0.90	14.81	309	4.31	1.02	2.01
V-3b	5-30	0.23	0.81	15.50	2.68	4.58	0.67	1.92

EF_i	Class 1 $EF_i<2$	Class 2 $2<EF_i<5$	Class 3 $5<EF_i<20$	Class 4 $20<EF_i<40$	Class 5 $EF_i>40$

According to PI$_i$ values (Table 9), soil is uncontaminated (Class 1) with Cd, Co, Cu (sites T-3b, T-4a, T-4b, T-5-a, T-5b, S-1a, S-1b, S-2b), Pb, and Zn (sites T-2b, T-3a, T-3b, T-4a, T-4b, T-5a, T-5b, T-6a, T-6b, S-1a, S-1b, S-2a, S-2b, V-1a, V-1b, V-2a, V-3b), low contaminated (Class 2) with Cu (sites T-1b, T-2a, T-2b, T-3a, S-2a, V-1a, V-1b, V-2a, V-2b, V-3a, V-3b), Ni (T-1a, T-1b, T-2b, T-4a, T-4b, T-5b, T-6a, T-6b, S-2a, S-2b, V-1a), and Zn (sites T-1a, T-1b, T-2a, V-2b, V-3a), moderate contaminated (Class 3) with Cr (site T-2b), Cu (site T-1a), Ni (sites T-2a, T-3a, T-3b, T-5a, S-1a, S-1b, V-2a, V-2b, V-3a, V-3b), high contaminated (Class 4) with Cr (sites T-1b, T-2a, T-3a, T-3b, T-4a, T-4b, T-5a, T-5b, V-1a, V-1b), and Cu (sites T-6a, T-6b), and very high contaminated (Class 5) with Cr (sites T-1a, T-6a, T-6b, S-1a, S-1b, S-2a, S-2b, V-2a, V-2b).

Table 9. PI_i values for the agricultural layers of soil in the Lower Danube Basin.

Sample site	Depth (cm)	PI_{Cd}	PI_{Co}	PI_{Cr}	PI_{Cu}	PI_{Ni}	PI_{Pb}	PI_{Zn}
T-1a	0-5	0.24	0.19	12.77	2.20	1.86	0.64	1.37
T-1b	5-30	0.23	0.49	4.96	1.89	1.92	1.00	1.23
T-2a	0-5	0.10	0.39	3.25	1.25	2.11	0.17	1.05
T-2b	5-30	0.11	0.36	2.78	1.26	1.79	0.30	0.98
T-3a	0-5	0.06	0.55	3.45	1.04	2.22	0.25	0.73
T-3b	5-30	0.05	0.54	3.51	0.97	2.08	0.24	0.65
T-4a	0-5	0.08	0.36	3.59	0.86	1.76	0.16	0.60
T-4b	5-30	0.09	0.36	3.71	0.89	1.83	0.20	0.67
T-5a	0-5	0.06	0.50	3.40	0.88	2.01	0.27	0.69
T-5b	5-30	0.05	0.53	3.66	0.86	1.75	0.34	0.67
T-6a	0-5	0.24	0.55	5.19	3.05	1.78	0.45	0.78
T-6b	5-30	0.26	0.57	5.85	3.41	1.74	0.32	0.76
S-1a	0-5	0.18	0.59	6.37	0.95	2.08	0.75	0.69
S-1b	5-30	0.14	0.59	6.12	0.95	2.07	0.74	0.63
S-2a	0-5	0.14	0.59	7.18	1.15	1.78	0.68	0.80
S-2b	5-30	0.13	0.63	6.84	0.99	1.81	0.67	0.71
V-1a	0-5	0.16	0.35	3.90	1.17	1.57	0.57	0.73
V-1b	5-30	0.16	0.33	4.11	1.23	1.51	0.49	0.73
V-2a	0-5	0.14	0.75	9.25	1.48	2.31	0.71	0.92
V-2b	5-30	0.15	0.67	11.65	1.71	2.78	0.67	1.04
V-3a	0-5	0.13	0.46	7.54	1.58	2.20	0.52	1.03
V-3b	5-30	0.11	0.38	7.25	1.25	2.14	0.32	0.90

PI_i	Class 1 $PI_i<1$	Class 2 $1<PI_i<2$	Class 3 $2<PI_i<3$	Class 4 $3<PI_i<5$	Class 5 $PI_i>5$

The soil enrichment risk, evaluated on the basis of PERI, is low for all the soil samples collected from Tulucesti, Sendreni and Vadeni (Table 10).

Table 10. PERI values for the agricultural layers of soil in the Lower Danube Basin.

Sample site	Depth (cm)	Er_{Cd}	Er_{Cr}	Er_{Cu}	Er_{Ni}	Er_{Pb}	Er_{Zn}	PERI
T-1a	0-5	7.07	25.54	10.99	9.30	3.19	2.73	58.82
T-1b	5-30	6.79	9.93	9.43	9.60	4.99	2.45	43.19
T-2a	0-5	3.04	6.51	6.26	10.54	0.84	2.09	29.27
T-2b	5-30	3.37	5.55	6.28	8.97	1.48	1.96	27.61
T-3a	0-5	1.80	6.89	5.19	11.11	1.23	1.46	27.67
T-3b	5-30	1.53	7.01	4.85	10.42	1.22	1.30	26.33
T-4a	0-5	2.53	7.18	4.28	8.82	0.80	1.21	24.82
T-4b	5-30	2.73	7.43	4.46	9.16	0.98	1.34	26.08
T-5a	0-5	1.82	6.80	4.38	10.05	1.35	1.39	25.79
T-5b	5-30	1.56	7.33	4.28	8.75	1.70	1.34	24.95
T-6a	0-5	7.14	10.38	15.27	8.90	2.23	1.57	45.49
T-6b	5-30	7.86	11.70	17.04	8.72	1.62	1.52	48.46
S-1a	0-5	5.27	12.73	4.74	10.39	3.77	1.39	38.30
S-1b	5-30	4.10	12.23	4.75	10.36	3.69	1.27	36.40
S-2a	0-5	4.27	14.36	5.73	8.89	3.41	1.59	38.25

S-2b	5-30	3.91	13.69	4.96	9.05	3.33	1.43	36.36
V-1a	0-5	4.72	7.81	5.84	7.83	2.83	1.46	30.49
V-1b	5-30	4.66	8.23	6.13	7.54	2.44	1.47	30.47
V-2a	0-5	4.06	18.49	7.41	11.55	3.56	1.83	46.91
V-2b	5-30	4.38	23.31	8.55	13.91	3.33	2.08	55.56
V-3a	0-5	3.80	15.09	7.88	10.98	2.59	2.05	42.39
V-3b	5-30	3.24	14.51	6.27	10.71	1.58	1.80	38.11

PERI	low potential risk PERI<150	moderate potential risk 150<PERI<300	high potential risk 300<PERI<600	very high potential risk PERI>600
Er_i	low risk Er_i <40	medium risk 40 < Er_i < 80	considerable risk 80 < Er_i < 160	high risk 160 < Er_i < 320	very high risk >320

The Contamination Severity Index (CSI) was used to evaluate the level of toxicity in the soil environment and identify any adverse impacts. The results for CSI (Table 11) indicated that overall, there was a very low level of soil contamination (Class 2). However, in specific sites such as T-1a, T-1b, S-1a, S-1b, and V-1a, the CSI values showed that the level of pollution was in the 3rd Class, indicating a low level of soil contamination.

Table 11. Soil level of contamination according to CSI and mERMQ indices.

Sample site	Depth (cm)	CSI_{Cd}	CSI_{Cr}	CSI_{Cu}	CSI_{Ni}	CSI_{Pb}	CSI_{Zn}	CSI	$mERM_Q$
T-1a	0-5	0.11	0.44	0.09	0.40	0.13	0.08	1.24	0.39
T-1b	5-30	0.11	0.20	0.08	0.41	0.17	0.07	1.04	0.28
T-2a	0-5	0.07	0.16	0.06	0.45	0.07	0.07	0.88	0.24
T-2b	5-30	0.08	0.14	0.07	0.39	0.09	0.06	0.82	0.22
T-3a	0-5	0.06	0.16	0.06	0.47	0.08	0.05	0.89	0.24
T-3b	5-30	0.05	0.16	0.06	0.44	0.08	0.05	0.85	0.23
T-4a	0-5	0.07	0.17	0.05	0.38	0.07	0.05	0.78	0.20
T-4b	5-30	0.07	0.17	0.05	0.39	0.07	0.05	0.81	0.21
T-5a	0-5	0.06	0.16	0.05	0.43	0.09	0.05	0.84	0.22
T-5b	5-30	0.05	0.17	0.05	0.38	0.10	0.05	0.80	0.21
T-6a	0-5	0.11	0.21	0.10	0.38	0.11	0.06	0.98	0.27
T-6b	5-30	0.12	0.23	0.11	0.38	0.09	0.06	0.98	0.27
S-1a	0-5	0.10	0.24	0.06	0.44	0.14	0.05	1.03	0.27
S-1b	5-30	0.08	0.23	0.06	0.44	0.14	0.05	1.01	0.27
S-2a	0-5	0.09	0.26	0.06	0.38	0.14	0.06	0.99	0.27
S-2b	5-30	0.08	0.25	0.06	0.39	0.13	0.05	0.97	0.26
V-1a	0-5	0.09	0.17	0.06	0.34	0.12	0.05	0.85	0.21
V-1b	5-30	0.09	0.18	0.06	0.33	0.12	0.05	0.84	0.21
V-2a	0-5	0.08	0.32	0.07	0.49	0.14	0.06	1.17	0.34
V-2b	5-30	0.09	0.40	0.08	0.60	0.13	0.07	1.36	0.41
V-3a	0-5	0.08	0.27	0.07	0.47	0.12	0.07	1.08	0.32
V-3b	5-30	0.08	0.27	0.07	0.46	0.09	0.06	1.02	0.30

CSI	Class 1 CSI<0.5	Class 2 0.5<CSI<1	Class 3 1<CSI<1.5	Class 4 1.5<CSI<2	Class 5 2<CSI<2.5	Class 6 2.5<CSI<3	Class 7 3<CSI<4	Class 8 4<CSI<5	Class 9 CSI>5

$mERM_Q$	Low risk $mERM_Q$<0.1	Medium risk 0.1<$mERM_Q$<0.5	High risk 0.5<$mERM_Q$<1.5	Very high risk $mERM_Q$>1.5

The mERMQ index was utilized to assess the potential for metal toxicity in the soil environment. The results for mERMQ (Table 11) show a relatively low risk, with a probability of toxicity estimated

at 9%. These findings reveal that the potential for metal toxicity in the soil ecosystem is not a significant cause for concern.

3.5. Major and Trace Elements Assessment in Crops

The study of toxic element contamination in crop plants is crucial for understanding the transfer of pollutants through the soil-plant system in agricultural areas located near industrial platforms. Knowing the concentrations of chemical elements in plants intended for human and animal consumption can help plan and implement measures to reduce the risk of contamination through the food chain.

The bioavailability and accumulation of heavy metals in plants depend on the physical, chemical, and biological properties of the soil [Arbanas (Moraru) S.-S. 2022]. Factors such as soil reaction, texture (especially colloidal clay), $CaCO_3$ content, and organic matter content influence the ion mobility of chemical elements [Smical, A.I. et al, 2008], [Kabata-Pendias, A., 2011]. Moreover, the level of bioaccumulation of metals varies depending on the species, vegetation stage, climatic, and relief conditions of the region where the plants grow. Some plants can be used as biomonitors for air, soil, and water, having the ability to accumulate toxic elements and metabolize them.

In recent years, experiments have been carried out on phytoremediation, which is the process of using plants to remove, degrade, or immobilize environmental contaminants [Krystofova, O. et al, 2009], [Gopal, R. and Khurana, N., 2011], [Dhiman, S.S. et al, 2017], [Mani, D. et al, 2012]. Sunflower has shown to be a good hyperaccumulator for toxic or potentially toxic elements such as Cr, Ni, Pb, Zn, Cu, and Cd. Under these conditions, crops must be monitored in terms of nutritional composition and potential elements with health risks, even in smaller quantities.

The analytical results for the level of heavy metals in wheat and corn grains and sunflower seeds (Table 12) comply with the maximum values provided in [Regulation (EC) no. 1881/2006], Codex Alimentarius [FAO/ WHO, 1995] and [Al-Othman, Z.A. et al, 2016] for certain contaminants in foodstuffs (Table 13). For Co, Cr, Cu, Ni, Pb, and Zn, European regulations do not provide a limit threshold in cereals and oilseeds. Similarly, no limit values are provided for heavy metals in the vegetative organs of cereals and sunflowers. If these plants are used in mixtures for animal feed, the concentrations of the mixture must not exceed the maximum permitted values provided in [Directive 2002/32/EC] on undesirable substances in feed, as amended.

Table 12. The heavy metals content in wheat, corn, and sunflower sections collected from agricultural lands in the Lower Danube Basin.

Plant sample	Plant species	Element (mg kg^{-1}±σ)						
		Cd	Co	Cr	Cu	Ni	Pb	Zn
T-1-l[1]	wheat	0.007±0.001	0.161±0.010	0.649±0.055	29.911±0.209	4.130±0.235	0.799±0.057	66.389±1.129
T-1-c		0.033±0.001	0.057±0.005	0.485±0.033	50.806±1.575	1.159±0.079	0.499±0.033	69.420±0.417
T-2-l	wheat	0.040±0.003	0.030±0.002	2.707±0.093	5.825±0.115	0.771±0.047	0.962±0.011	62.613±0.771
T-2-c		0.046±0.003	0.009±0.001	0.801±0.050	8.218±0.177	0.680±0.019	0.640±0.059	66.211±0.357
T-3-l	corn	0.093±0.001	0.038±0.001	2.386±0.071	20.539±0.270	0.885±0.094	0.774±0.035	69.307±0.875
T-3-c		0.012±0.001	0.008±0.001	0.547±0.052	3.076±0.017	0.718±0.034	0.217±0.015	22.385±1.244
T-4-l	corn	0.056±0.002	0.050±0.003	2.501±0.011	22.779±0.307	1.147±0.001	1.461±0.039	78.468±0.233
T-4-c		0.003±0.001	0.003±0.001	0.246±0.016	1.268±0.074	0.094±0.065	0.051±0.003	19.672±0.493
T-5-l	sun flower	0.180±0.006	0.021±0.002	0.641±0.006	11.859±0.073	0.511±0.023	0.955±0.030	28.243±0.934
T-5-a		0.400±0.004	0.010±0.001	0.103±0.010	28.958±0.230	6.816±0.144	0.372±0.034	84.504±0.149
T-6-l	sun flower	0.171±0.005	0.022±0.001	0.714±0.039	86.089±0.863	0.929±0.075	0.805±0.036	30.439±0.537
T-6-a		0.132±0.002	0.012±0.001	2.095±0.055	54.319±0.363	3.869±0.087	0.314±0.014	74.133±1.469
S-1-l	wheat	0.004±0.001	0.563±0.015	2.702±0.024	13.536±0.122	3.401±0.024	1.413±0.008	40.903±1.595

S-1-c		0.000±0.000	0.020±0.001	0.100±0.004	20.224±0.263	0.400±0.034	0.026±0.002	47.584±1.570
S-2-l	sun	0.174±0.007	0.076±0.005	0.443±0.017	535.348±0.535	2.020±0.125	0.007±0.001	56.720±0.397
S-2-a	flower	0.114±0.001	0.047±0.004	0.711±0.033	120.146±8.290	5.471±0.350	0.645±0.40	69.433±1.180
V-1-l	wheat	0.001±0.001	0.195±0.016	1.623±0.067	25.968±1.195	3.670±0.194	0.714±0.052	31.842±0.318
V-1-c		0.001±0.001	0.062±0.005	0.332±0.009	58.397±0.467	1.164±0.115	0.383±0.022	51.620±0.723
V-2-l	sun	0.320±0.023	0.128±0.011	0.042±0.002	318.245±8.911	1.187±0.078	0.009±0.001	131.596±2.106
V-2-a	flower	0.224±0.007	0.038±0.004	1.333±0.041	80.496±0.724	3.797±0.106	1.282±0.054	81.263±0.975
V-3-l	sun	0.361±0.007	0.119±0.009	0.428±0.001	235.947±6.842	5.005±0.445	0.011±0.001	144.851±2.028
V-3-a	flower	0.246±0.002	0.030±0.002	0.832±0.007	89.742±1.346	4.653±0.167	1.542±0.140	95.135±0.856

[1] l-leaves; c-caryopsis; a-achenes.

Table 13. The maximum permissible levels of heavy metals in the grains and seeds of wheat, corn, sunflower, and crops according to different authors.

Product	Element (mg kg^{-1})							References
	Cd	Co	Cr	Cu	Ni	Pb	Zn	
Wheat and corn grains	0.10	-	-	-	-	0.20	-	[Regulation (EC) no. 1881/2006]-[https://eur-lex.europa.eu/homepage.html]
Sunflower seeds	0.50	-	-	-	-	0.10	-	[FAO/WHO, 1995]
Crops	0.20	-	2.30	73.30	67.90	0.30	99.40	[Al-Othman, Z.A. et al, 2016]

Cadmium in Plants

The concentration of Cd in *wheat* varies between 0.001±0.001 and 0.040±0.003 mg kg^{-1} d.w. in leaves and between 0.000±0.000 and 0.046±0.003 mg kg^{-1} d.w. in caryopsis. The average content of Cd in caryopsis falls within the [FAO/WHO, 1995] and [Al-Othman, Z.A. et al, 2016] recommendations for all sampling sites. [Kabata-Pendias, A., 2011] reports average values of Cd in wheat grains, grown under various conditions, of 4.5-270.0 mg kg^{-1}. [Yang, Y. et al, 2014] shows that Cd accumulation in plants occurs in the order root>stem>grain when applying Cd treatments in different concentrations to the soil in wheat and corn. The present study confirms the higher accumulation in leaves than in grains (site S-1), but higher concentration in grains than in leaves (sites T-1, T-2). Therefore, careful monitoring of this crop is required due to the tendency of transfer of Cd in grains.

In *corn*, the average content of Cd is present within the limits of 0.056±0.002- 0.093±0.001 mg kg^{-1} d.w., in leaves, and between 0.003±0.001 and 0.012±0.001 mg kg^{-1} d.w., in caryopsis. These values fall within the maximum permissible limit recommended by [Regulation (EC) no. 1881/2006] and [FAO/WHO, 1995]. [Yang, Y. et al, 2014] shows that Cd accumulates in large quantities in the root and stem at increasingly high concentrations of Cd in the soil, unlike the grain, which makes corn able to be used as a hyperaccumulator in polluted areas, without posing risks to consumers, provided that the contaminated tissues are not used for animal feed.

In *sunflower*, Cd varies in the range 0.171±0.005-0.361±0.007 mg kg^{-1} d.w. in the leaves and 0.114±0.001-0.400±0.004 mg kg^{-1} d.w. in achenes. The values do not exceed the maximum permissible limit for Cd, established by [Regulation (EC) no. 1881/2006] and [FAO/WHO, 1995]. [Gopal, R. and Khurana, N., 2011] shows that sunflower accumulates Cd more in the root, and the concentration of this element in the plant decreases in the order root>stem>leaves. At the same time, the study of [Alaboudi, K. et al, 2018] on the ability of sunflower to phytoextract Cd, shows that it is a good hyperaccumulator of this element, especially at the root level.

Cobalt in Plants

The concentration of Co in *wheat* lies in the range of 0.030±0.002-0.563±0.015 mg kg^{-1} d.w. in leaves and 0.009±0.001-0.062±0.005 mg kg^{-1} d.w. in caryopsis. The highest concentration of Co in leaves was found at sampling site S-1, located near the slag dump. In *corn*, the concentration of Co ranges from 0.038±0.001 to 0.050±0.003 mg kg^{-1} d.w. in leaves and 0.003±0.001-0.008±0.001 mg kg^{-1} d.w. in caryopsis. The accumulation of Co in *sunflower* follows a similar trend as in wheat and corn, with an average Co content ranging from 0.021±0.002-0.128±0.011 mg kg^{-1} d.w. in the leaves and 0.010±0.001-0.047 ±0.004 mg kg^{-1} d.w. in achenes.

In Europe, no maximum threshold has been established for the concentration of Co in cereals and sunflower seeds. The present study shows that Co accumulates in the order of leaf > caryopses/achenes. Other studies have reported the following concentrations of Co in crop plants: 0.14-0.49 mg kg^{-1} in wheat grains [Tegegne, W.A., 2015], [Shobha, N. and Kalshetty, B.M., 2017], and 0.15-0.24 mg kg^{-1} in corn grains [Tegegne, W.A., 2015], [Antoniadis, V. et al. a., 2019].

Chromium in Plants

The results on *wheat* sections found that Cr tends to accumulate in larger amounts in the leaves, with values ranging from 0.649±0.055 to 2.707±0.093 mg kg-1 d.w. In caryopsis, the concentration was between 0.100±0.004 and 0.801±0.050 mg kg^{-1} d.w. The highest concentrations of Cr were found in sampling sites T-2 (Tulucesti), S-1 (Sendreni), and V-1, (Vadeni). The results suggest that the concentration of Cr in different parts of the wheat plant is influenced by the ecological conditions in which the plants grow.

In *corn*, the highest concentrations of Cr were found in the leaves, with concentrations ranging from 2.386±0.0071 to 2.501±0.011 mg kg^{-1} d.w., while in caryopsis, the concentration ranged from 0.246±0.016 to 0.547±0.052 mg kg^{-1} d.w. The average value of Cr in leaves and corn grains was 2.077 mg kg^{-1} and 0.361 mg kg^{-1}, respectively, when cultivated on soils fertilized with sewage sludge [Liang, J. et al, 2011].

Sunflower showed a different trend of Cr accumulation, with the highest values recorded in the achenes (0.711±0.033 to 2.095±0.055 mg kg^{-1} d.w.), whereas in the leaves, this element was found in concentrations of 0.042±0.002 to 0.714±0.039 mg kg^{-1} d.w. [Liang, J. et al, 2011] suggests that both corn and sunflower are good accumulators of Cr, particularly in the root. According to his study, the concentration of Cr decreases in the following order: root > stem > leaves > achenes for sunflower and root > leaves > stem > caryopsis for corn. There are no regulated maximum values allowed for total Cr in the edible sections of crops. However, according to the study conducted by [Al-Othman, Z.A. et al. 2016], the maximum allowed value of Cr in crops is 2.30 mg kg^{-1}.

Copper in Plants

In *wheat*, the leaves recorded the lowest average values ranging from 5.825±0.115 to 25.968±1.195 mg kg^{-1} d.w., while the average level of Cu in caryopsis ranged from 8.218±0.177-58.397±0.467 mg kg^{-1} d.w. This indicates that the concentration of Cu in wheat is higher in the caryopsis than in the leaves.

In *corn*, the concentration of Cu was found to be higher in the leaves, with an average concentration of 20.539±0.0270-22.779±0.307 mg kg^{-1} d.w. compared to caryopsis, where the values were within 1.268±0.074-3.076±0.017 mg kg^{-1} d.w. This demonstrates that the distribution of Cu in corn varies between leaves and caryopsis.

In the case of *sunflowers*, the samples taken from Tulucesti territory have an average concentration of Cu in leaves ranging from 11.859±0.073 to 86.089±0.863 mg kg^{-1} d.w. In achenes, the concentration varies between 28.958±0.230-54.319±0.363 mg kg^{-1} d.w., with the maximum value recorded at sampling site I-6. The average Cu content in leaves is 535.348±0.535 mg kg^{-1} d.w. in Sendreni, and in Vadeni, it varies between 235.947±6.842 and 318.245±8.911 mg kg^{-1} d.w. In achenes, Cu ranges between 80.496±0.724 and 120.146±8.290 mg kg^{-1} d.w., with a maximum at sampling site S-2. The distribution of Cu in sunflowers varies significantly depending on the location and the agricultural chemical treatments of the plant.

The concentration of Cu in *wheat* and *corn* was found to be below the maximum limit recommended by [Al-Othman, Z.A. et al, 2016] for crops, which is 73.30 mg kg^{-1}. However, in *sunflowers*, the concentration of Cu exceeded the limit in some cases. The maximum permissible limits of Cu content regulated in Europe for sunflower seeds are not defined. Therefore, the results for sunflowers indicate the need for further research to determine the safe limits of Cu content in sunflower seeds. According to [Kabata-Pendias, A., 2011], the range 20-100 mg kg^{-1} can be used to assess the Cu toxicity threshold of plants.

Nickel in Plants

The analytical data obtained for *wheat* shows that the concentration of Ni is higher in the leaves compared to the caryopses. The average Ni concentration in the leaves ranges from 0.771±0.047 to 4.130±0.235 mg kg^{-1} d.w., while in the caryopses it ranges from 0.400±0.034-1.164±0.115 mg kg^{-1} d.w.

Similarly, for *corn*, the average Ni concentration is higher in the leaves compared to the caryopses. The average Ni concentration in the leaves ranges from 0.885±0.094- 1.147±0.001 mg kg^{-1} d.w. and in the caryopses, it ranges from 0.094±0.065-0.718±0.034 mg kg^{-1} d.w.

On the other hand, in the case of *sunflowers*, the Ni concentration is higher in the achenes than in the leaves. The average Ni concentration in the achenes ranges from 3.797±0.106-6.816±0.144 mg kg^{-1} d.w., while in the leaves, it ranges from 0.511±0.023- 5.005±0.445 mg kg^{-1} d.w.

It's worth noting that there are no established maximum allowed values for Ni in cereals and oilseeds in EU. However, according to [Al-Othman, Z.A. et al, 2016], the Ni concentration in crops should not exceed the threshold of 67.90 mg kg^{-1}. The results obtained in this analysis indicate that the Ni concentration in the analyzed plants is below the recommended above mentioned threshold.

Lead in Plants

The analytical results revealed that Pb accumulation in *wheat* leaves is higher than in caryopses, with values ranging from 0.714±0.052 to 1.413±0.008 mg kg^{-1} d.w. for leaves and 0.026±0.002 to 0.640±0.059 mg kg^{-1} d.w. for caryopses. The average concentrations for caryopses exceed the maximum value set by [Regulation (EC) no. 1881/2006] and [FAO/WHO, 1995].

Similarly, the average values of Pb in *corn* are higher in the leaves, ranging from 0.774±0.035 to 1.461±0.039 mg kg^{-1} d.w., compared to those in the caryopsis, where they vary from 0.051±0.003 to 0.217±0.015 mg kg^{-1} d.w. Notably, the average values of Pb at the T-3 site (Tulucesti) exceed the permissible limit of 0.20 mg kg^{-1}. However, for all caryopsis samples, the lead level is below the values recommended by [Al-Othman, Z.A. et al, 2016]. According to [Liang, J. et al. a., 2011], lead accumulation is usually higher in the roots than in the leaves and grains.

Regarding *sunflower* sections, two distinct situations were found. In the Tulucesti territory, the study revealed higher Pb accumulation in the leaves, with average concentrations ranging from 0.805±0.036 to 0.955±0.030 mg kg^{-1} d.w., than in the achenes, where average values were between 0.314±0.014 to 0.372±0.034 mg kg^{-1} d.w. In contrast, in the territories of Sendreni and Vadeni, Pb registers higher average values in the achenes, ranging from 0.646±0.400 to 1.542±0.140 mg kg^{-1} d.w., compared to those in the leaves, which ranged from 0.007±0.001 to 0.011±0.001 mg kg^{-1} d.w. The average concentration of Pb in achenes collected from these territories exceeds the maximum allowed value established by [Regulation (EC) no. 1881/2006] and [FAO/WHO, 1995], as well as the value mentioned by [Al-Othman, Z.A. et al, 2016]. However, [Alaboudi, K. et al. a., 2018] revealed that sunflowers are good accumulators of this element, and [Zehra, A. et al. 2020] concluded that the quality of the obtained oil does not exceed food safety regulations, despite the high content of Pb extracted by the plant. [Liang, J. et. Al. 2011] suggests that lead transfer in sunflower sections occurs in the order root>stem>leaves>achenes, which is confirmed by the present study for the Tulucesti territory, while for Sendreni and Vadeni, the situation is the opposite.

Zinc in Plants

In *wheat*, it was found that the caryopsis had a tendency to accumulate more zinc than the leaves. The concentration of zinc in caryopses ranged from 47.584±1.570 to 69.420±0.417 mg kg⁻¹ d.w., while in leaves it varied between 31.842±0.0.318 and 66.389±1.129 mg kg⁻¹ d.w. It was observed that the concentration of zinc in caryopses was below the maximum limit mentioned in [Al-Othman, Z.A. et al. 2016].

In *corn*, it was found that the leaves accumulated more zinc than the caryopsis. The average concentration of zinc in leaves ranged from 69.307±0.875 to 78.468±0.233 mg kg⁻¹ d.w., while in caryopsis it was between 19.672±0.493-22.385±0.1.244 mg kg⁻¹ d.w. The concentration of zinc in corn was below the value mentioned by [Al-Othman, Z.A. et al. 2016].

Finally, in *sunflower*, the concentration of zinc was observed to be higher in achenes than in leaves, except for sampling points V-2 and V-3 (Vadeni), where the situation was opposite. The average concentration of zinc in leaves ranged from 28.243±0.934 to 144.851±2.028 mg kg⁻¹ d.w., while in achenes it ranged from 69.433±1.180 to 95.135±0.856 mg kg-1 d.w. There are no EU maximum permissible limits of zinc for sunflower seeds, but the values recorded in achenes were lower than 99.40 mg kg⁻¹ [Al-Othman, Z.A. et al. 2016].

Other Trace Elements in Plants

The PIGE method has proven to be a highly effective tool for identifying various elements that play a crucial role in the plant growth and development. This method has enabled the identification of a range of essential or toxic elements, including F, Na, Mg, Fe, Al, P, Si, Mg, and Cl. The chemical composition of plants provides vital insights into their growth and development, revealing a close association with the soil on which they are cultivated. Table 14 presents the elemental concentration in plant sections.

Table 14. The content of macro and microelements in wheat, corn and sunflower plants collected from the Lower Danube Basin.

Plant sample	Plant species	Element (mg kg⁻¹±σ)							
		F	Na	Mg	Al	Si	P	Cl	Fe
T-1-l[1]	wheat	17±6	830±20	9870±867	748±48	61300±5500	3870±220	n.d.	3940±1110
T-1-c		<18	120±20	4441±1314	<140	<16900	4750±490	n.d.	<4420
T-2-l	wheat	270±3	1440±26	8019±632	2850±90	155000±9800	2070±190	<1300	4990±930
T-2-c		<16	290±30	4251±1675	<140	<15800	2290±290	n.d.	<4280
T-3-l	corn	23±4	1156±30	8249±806	2543±100	110190±7284	2234±174	<1205	5463±1012
T-3-c		<10	26±10	<2222	<78	<9022	2287±293	n.d.	3871±1382
T-4-l	corn	30±5	616±28	21802±1859	2530±98	122881±7820	6436±300	<1215	6302±1289
T-4-c		10±4	21±8	4481±2008	460±74	<8634	3438±264	n.d.	<2418
T-5-l	sun flower	9±3	241±16	66761±3379	1159±73	22276±3640	6862±306	<1380	5472±1094
T-6-l	sun flower	15±3	228±13	30532±2015	855±62	35195±4448	4629±263	3071±703	4879±1003
S-1-l	wheat	18±3	741±30	5043±642	1693±76	77847±7695	695±131	n.d.	<2109
S-1-c		<10	20±6	1812±198	120±31	<10031	1041±139	n.d.	<2381
S-2-l	sun flower	<12	71±13	19701±2699	245±83	19500±5967	2486±356	18915±1495	6347±2317
V-1-l	wheat	<13	1342±42	4029±1078	1122±102	80858±15848	1517±320	4029±1078	3521±1556
V-1-c		10±4	47±14	<1977	<90	<11532	1623±261	<1977	<3107
V-2-l	sun flower	13±4	124±19	17414±2155	286±60	12678±3410	2431±294	19254±1240	10133±1900

Plant sample	Plant species	Element (mg kg^{-1}±σ)							
		F	Na	Mg	Al	Si	P	Cl	Fe
V-3-l	sun flower	19±6	192±25	24557±2701	383±84	<17525	1686±403	29102±1647	7952±1606

[1] l-leaves; c-caryopsis; a-achenes; n.d. - not detected.

3.6. The Organic Compounds Found in Crops

Plant tissues are intricate and fascinating structures that consist of a complex combination of organic compounds. These compounds, which include cellulose, lignins, sugars, proteins, starch, lipids, and wax, play a crucial role in the development of various physiological processes in plants, as well as in the nutrition of humans and animals who consume these plants. To better understand the properties and functions of these organic compounds, Table 15 provides a detailed breakdown of the absorption bands associated with the functional groups found in the analyzed plant tissues, presented in Figure 8.

Table 15. The absorption bands linked with vibrations functional group of organic compounds in selected plant samples collected from the Lower Danube Basin [Arbanas (Moraru) S.-S. 2022].

Absorption band (cm^{-1})		Band assignment[1]	Reference
Wheat leaves	Sunflower leaves		
3293	3273	ν (≡C-H): alchine $\nu(-(C)O-H)$: alcohols, phenols ν (-(C)-N-H): Amine I	3270-3330 cm^{-1} ν (≡C-H) [*] 3200-3550 cm^{-1} $\nu(-(C)O-H)$ [*] 3200-3500 cm^{-1} ν (-(C)-N-H) [*]
2918, 2850	2918, 2850	$\nu_{as/sym}(CH_2)$: lipids, together with proteins, carbohydrates, and nucleic acids $\nu(-(C)O-H)$: carboxylic acids $\nu(-(C-H))$: alkane	2959-2852 cm^{-1} $\nu_{as}(CH_2)$ [Demir, P. et al, 2015], 2920 cm^{-1} $\nu_{sym}(CH_2)$ [Utami, S.N.H. and Suswati, D., 2016] 2852 cm^{-1} $\nu_{sym}(CH_2)$ [Gorgulu, S.T. et al, 2007] 2500-3300 cm^{-1} $\nu(-(C)O-H)$ [*] 2800-3000 cm^{-1} $\nu(-(C-H)$ [*]
1729	1731	$\nu(-C=O)$: carboxylic acids $\nu(C=O)$ of esters : phospholipids, cholesterol esters, hemicellulose, and pectin	1680-1760 cm^{-1} $\nu(-C=O)$ [*],[Utami, S.N.H. and Suswati, D., 2016] 1733 cm^{-1} $\nu(C=O)$ [Gorgulu, S.T. et al, 2007]
1637	1597	$\nu_{as}(C=O)$: proteins, lignins $\nu(-C=C-)$: phenols β (-(C)-N-H): Amine I	1650-1600 cm^{-1} $\nu_{as}(C=O)$ [Utami, S.N.H. and Suswati, D., 2016], 1550-1700 cm^{-1} $\nu(-C=C-)$ [*] 1500-1650 cm^{-1} β (-(C)-N-H) [*]
1419	1403	$\beta(OH)$: polysaccharides, alcohols, carboxylic acids $\beta(-C-H)$: alkane	1414 cm^{-1} $\beta(OH)$ [Demir, P. et al, 2015] 1395-1440 cm^{-1} $\beta(-(C)O-H)$ [*] 1400-1470 cm^{-1} $\beta(-C-H)$ [*] 1415 cm^{-1} $\beta(OH)$ [Gorgulu, S.T. ş.a., 2007]
1374	-	$\beta(CH_2)$: hemicellulose, xyloglucans, phenols and aliphatic structures $\beta(-(H)_2C-H)$: alkane	1350-1380 cm^{-1} $\beta(-(H_2C-H)$ [*] 1371 cm^{-1} $\beta(C-H)$ [Utami, S.N.H. and Suswati, D., 2016]

Absorption band (cm^{-1})		Band assignment[1]	Reference
Wheat leaves	Sunflower leaves		
1317	1322	$\beta(CH_2)$: cellulose $\nu(-C-OH)$: carboxylic acids $\nu(C-OH)$: phenols	1369, 1335, 1315, 1280 cm^{-1} $\beta(CH_2)$ [Demir, P. et al, 2015] 1210-1320 cm^{-1} $\nu(-C-OH)$ [*] 1310-1390 cm^{-1} $\nu(C-OH)$ [*]
-	1240	Amine III $\nu(C-N)$; $\nu(N-H)$: proteins $\nu(-C-OH)$: carbohylic acid $\nu(-C-F)$: akyl fluoride $\nu(-S=O)$: sulfoxide	1239 cm^{-1} $\nu(C-N)$; $\nu(N-H)$ [Demir, P. et al, 2015] 1235 cm^{-1} $\nu(C-N)$; $\nu(N-H)$ [Gorgulu, S.T. ș.a., 2007] 1210-1320 cm^{-1} $\nu(-C-OH)$ [*] 1000-1400 cm^{-1} $\nu(-C-F)$ [*] 1030-1372 cm^{-1} $\nu(-S=O)$ [*]
1033	1025	$\nu(C-O)$; $\beta(OH)$: polysaccharides, , xyloglucans $\nu(-C-N-)$: Amine I, II, III $\nu(-C=S)$: thioketone	1035 cm^{-1} $\nu(-C-N-)$ [Gorgulu, S.T. ș.a., 2007] 1020-1200 cm^{-1} $\nu(-C-N-)$ [*] [Demir, P. et al, 2015] 1000-1250 cm^{-1} $\nu(-C=S)$ [*]
784	-	$\beta(-(C)-N-H)$: Amine I, II $\beta(C-H)$: phenols	660-900 cm^{-1} $\beta(-(C)-N-H)$ [*] 680-860 cm^{-1} $\beta(C-H)$ [*]
-	535	$\nu(-C-I)$, $\nu(-C-Br)$: alkyl iodide and alkyl bromide	500-600 cm^{-1} $\nu(-C-I)$ [*] 515-690 cm^{-1} $\nu(-C-Br)$ [*]

[1] ν-stretching vibration, $\nu_{as/sim}$-asymmetric/ symmetric stretching vibration, β- bending vibration; [*][https://specac.com] .
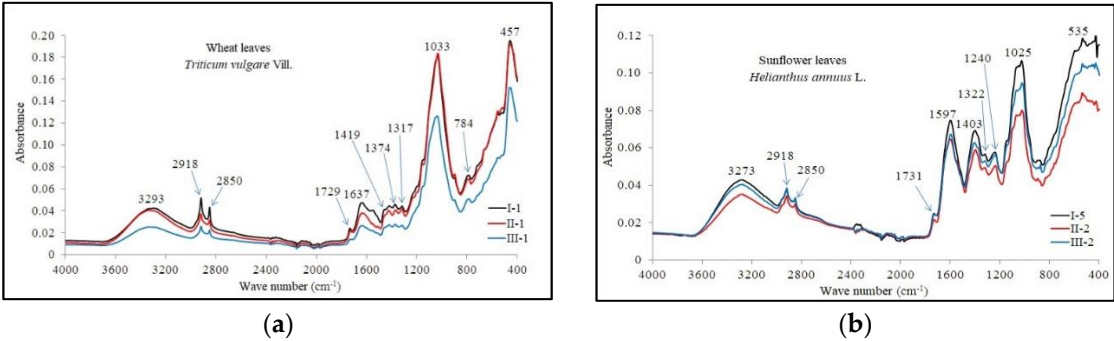
Figure 8. ATR-FTIR characteristic spectra of: (**a**) wheat and (**b**) sunflower leaves.

The plant tissues of the analyzed plants were found to contain several functional groups, including alkynes, alcohols, phenols, and amines I and II, identified by intense peaks in the area 3293 cm^{-1} and 3273 cm^{-1}. These peaks are attributed to the stretching vibrations of groups such as ≡C-H, -(C)O-H, and -(C)-N-H [*]. The presence of lipids, proteins, carbohydrates, and nucleic acids was also indicated by strong peaks recorded at wavenumbers 2918 cm^{-1} and 2850 cm^{-1}, attributed to symmetric and asymmetric vibrations of carboxylic acids (-C=O) and alkanes (C-H). [Demir, P. et al., 2015], [Utami, S.N.H. and Suswati, D., 2016] and [Gorgulu, S.T. et al., 2007] mention these groups at 2959-2852 cm^{-1}, 2920 cm^{-1} and 2852 cm^{-1}.

The wheat leaves showed much more pronounced peaks compared to those identified in the spectrum of sunflower leaves. A peak at 1733 cm^{-1} was attributed to the stretching vibration of the C=O group in the structure of carboxylic acids, phospholipids, hemicellulose, and pectin [Gorgulu, S.T. et al., 2007], which were identified in the spectra of analyzed wheat and sunflower leaves at wave

numbers 1729 cm^{-1} and 1731 cm^{-1}. These functional groups were also identified in the range of 1760-1680 cm^{-1} [Utami, S.N.H. and Suswati, D., 2016].

In the ATR-FTIR spectra of plant leaves, the absorption bands between 1650-1500 cm^{-1} range are attributed to the stretching vibrations of primary amines, proteins, lignins and phenols. The peaks at 1637 cm^{-1} (wheat leaf) and 1597 cm^{-1} (sunflower leaf) signify the presence of primary amines. Additionally, the absorption band within 1470-1400 cm^{-1} range is attributed to the deformation vibration of C-OH and C-H groups found in polysaccharides, alcohols, carboxylic acids, and alkanes. The peaks at 1419 cm^{-1} (wheat leaf) and 1403 cm^{-1} (sunflower leaf) indicate the presence of these functional groups. The wave number 1317 cm^{-1} is attributed to the deformation vibration of the CH group in the cellulose structure and the stretching vibrations of C-OH groups in carboxylic acid and phenols. These peaks were observed in the ATR-FTIR spectrum at wave numbers 1317 cm^{-1} and 1322 cm^{-1}. The absorption band at 1374 cm^{-1} is attributed to the deformation vibration of CH and H$_2$C-H groups found in hemicellulose, xyloglucans, alkanes, phenols, and aliphatic structures. These clusters [*] were detected in wavenumbers 1380-1350 cm^{-1} and 1371 cm^{-1} [Utami, S.N.H. and Suswati, D., 2016].

The region spanning from 1240 to 1033 cm^{-1} is indicative of polysaccharides, xyloglucans, and primary, secondary, and tertiary amines. The absorption bands in this range are associated with the stretching vibrations of the C-N, N-H, and C-O groups, as well as the deformation vibrations of the OH group within their structure [Gorgulu, S.T. et al, 2007], [Demir, P. et al, 2015]. Of particular note are the highly intense peaks at 1033 cm^{-1} in the wheat leaf spectrum, and at 1025 cm^{-1} in the sunflower leaf spectrum.

Amines I and II, along with phenols, are identified in the spectrum obtained from wheat leaves by the average intensity peak at wave number 784 cm^{-1}, which is associated with the deformation vibration of C-N-H and C-H groups. The presence of these groups is noted [*] in the range of 900-660 cm^{-1} and 860-680 cm^{-1}. Furthermore, the peak at wave number 535 cm^{-1}, exclusive to the spectrum of sunflower leaves, is indicative of the stretching vibrations of the C-I and C-Br groups found in the alkyls within the plant's structure.

In Figure A2, Appendix A, SEM micrographs (5,000x), EDX spectra and elemental mapping of wheat and corn caryopsis, as well as sunflower achenes from various locations including Tulucesti and Sendreni in Galați County, and Vadeni in Braila County are presented. The micrographs depict the structural elements of plant tissues, such as cell walls, membranes, and organic substances like lipids, starch, and proteins. Additionally, the Table A2 (Appendix A), along with the EDX spectra and elemental distribution, revealed the presence of a number of 23 macro-, micro-, and trace elements in the grains and achenes, similar to those found in the soil. These findings underscore the strong relationship between soil mineralogy and plant composition. The grain tissue components with physiological activity are clearly marked and easily identifiable based on their morphology according [Heneen, W.K. and Brismar, K., 1987], [Shorstkii, I.A. et al, 2019], [Scheuer, P.M. et al, 2011].

3.7. The Bioaccumulation of Elements in Crops

The Bioconcentration Factors (BFs) of soil heavy metals in crop plant leaves and caryopsis/achenes are shown in Figure 9 and Figure 10.

The results indicate that, in the agroecological conditions of the studied area, *wheat* plants tend to exclude the bioaccumulation of Cd, Co, Cr, Ni, and Pb in their tissues. BFs for Cd ranged from 0.01 to 0.38 for leaves and from 0.00 to 0.43 for caryopsis. BFs for Co were between 0.01 and 0.06 for leaves and from 0.00 to 0.01 for caryopsis. The lowest BFs were observed for Cr (0.00-0.03 for leaves and 0.00-0.01 for caryopsis). BFs for Ni ranged between 0.02 and 0.11 for leaves and from 0.01 to 0.04 for caryopsis. BFs for Pb ranged from 0.07 to 0.21 for leaves and from 0.00 to 0.14 for caryopsis. In contrast, for Zn and Cu, the bioaccumulation pattern was different. While the trend for the other elements was leaves > caryopsis, for Zn and Cu, it was caryopsis > leaves. BFs for Zn ranged from 0.43 to 0.62 for leaves and from 0.54 to 0.72 for caryopsis. The bioaccumulation of Cu was particularly pronounced in caryopsis, with BFs ranging from 0.23 to 1.09 for leaves and from 0.33 to 2.44 for caryopsis.
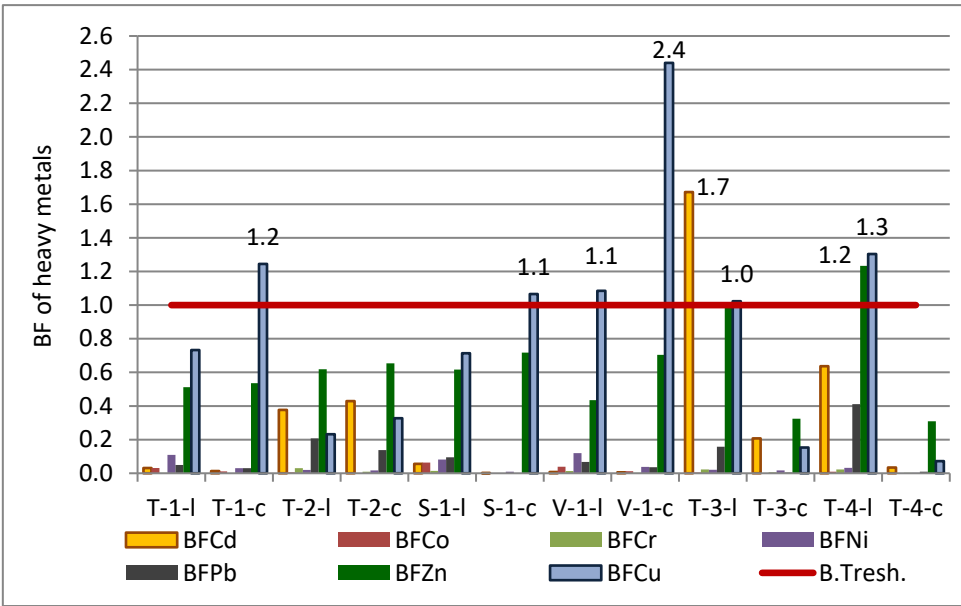
Figure 9. Bioaccumulation factor of heavy metals in wheat and corn leaves and caryopsis.

In the case of corn leaves and caryopses, the bioaccumulation factor for most elements was below 1 (the bioaccumulation threshold - B.Tresh.), indicating a limited capacity for phytoaccumulation under the ecological conditions in which the corn was grown. However, exceptions were observed for Cd, Zn, and Cu, with BFs exceeding 1, suggesting a tendency for bioaccumulation of these elements in the leaves. Comparing the sections of the corn plant, the overall order of bioaccumulation was from leaf to caryopsis. Specifically, the BFs in leaves followed the order: Cd (0.64-1.67) > Zn (1.00-1.23) > Cu (1.02-1.30) > Pb (0.16-0.41) > Ni (0.02-0.03) > Cr (0.02) > Co (0.00-0.01), while in the case of caryopses, the order of bioaccumulation was Zn (0.31-0.32) > Cd (0.03-0.21) > Cu (0.07-0.15) > Ni (0.00-0.02) > Cr=Pb (0.00-0.01) > Co (0.00).
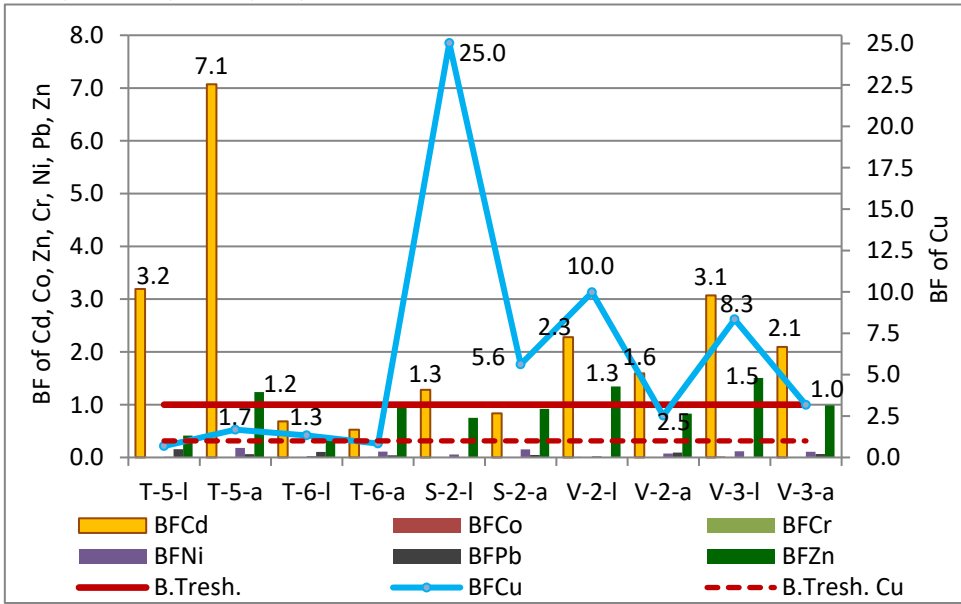
Figure 10. Bioaccumulation factor of heavy metals in sunflower leaves and achenes.

The results for sunflower BFs indicate that the bioconcentration of Cu, Cd, and Zn in both the leaves and achenes (seeds) is higher than that of other elements. The highest bioaccumulation values are observed for Cu, which in the sampling sites S-2, V-2, and V-3 show the most significant accumulation. Specifically, for leaves, the bioaccumulation factor decreases in the order: Cu (0.69-25.0279) > Cd (0.68-3.19) > Zn (0.39-1.50) > Pb (0.00-0.16) > Ni (0.01-0.12) > Co (0.00-0.02) > Cr (0.00-

0.01), while for achenes the order is: Cd (0.53-7.07) > Cu (0.84-5.62) > Zn (0.83-1.24) > Ni (0.07-0.18) > Pb (0.04-0.09) > Cr=Co (0.00-0.01).

Corn and sunflower, as high biomass-producing plants, exhibit a notable capacity for the bioaccumulation of heavy metals in comparison to wheat. This study presents evidence indicating that corn and sunflower demonstrate a greater susceptibility for the bioextraction of copper, zinc, and cadmium.

3.8. Health Risk Assessment

The hazard quotient values for the three pathways of exposure (ingestion, dermal contact, and inhalation) indicate that there is no potential risk of adverse health effects for the adult population when exposed to Cr, Pb, Co, Zn, Cd, Ni, and Cu. The noncarcinogenic risks calculated for children also show no potential adverse effects from exposure to the investigated heavy metals, except for Cr. In two locations from Tulucesti and Vadeni, the dermal contact hazard quotient for Cr was greater than 1 (T-1 - 1.17, V-2 - 1.38), indicating a potential risk for adverse health effects in these areas.

According to the HQ results, it has been found that human exposure to Co may occur through ingestion for both adults (0.01-0.02) and children (0.15-0.32), but risk is negligible. On the other hand, exposure to Cr may occur through dermal contact and ingestion. The HQ for dermal and ingestion exposure in children is higher than that in the adult population. Specifically, the HQ for dermal exposure ranges from 0.40 to 1.38 for children and from 0.04 to 0.15 for adults. Similarly, the HQ for ingestion ranges from 0.28 to 0.95 for children and from 0.02 to 0.07 for adults. It's important to note that Pb, Zn, Cd, Ni, and Cu do not pose any hazardous risk for either children or adults. However, in Vadeni and some sites in Tulucesti (T-1, T-2, T-6), the HQ ingestion for Cu recorded very low levels (0.01).

The HI values for Co ranged from 0.01 to 0.02 for adults and from 0.15 to 0.32 for children. In contrast, Cr poses a higher risk of adverse health effects for children, with HI values ranging from 0.67 to 2.34, compared to 0.06 to 0.22 for adults. This suggests that children may be more vulnerable to exposure through ingestion, as they often put unwashed hands and objects they play with in their mouths. The health risk level by exposure to Cr and Co is presented in Figure 11.
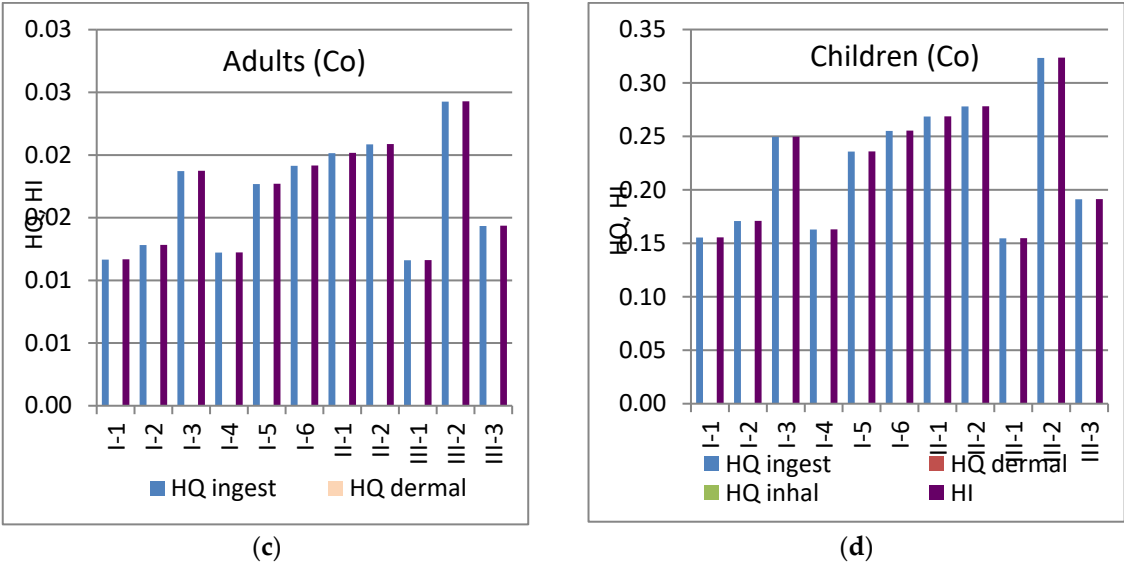

(**a**)   (**b**)
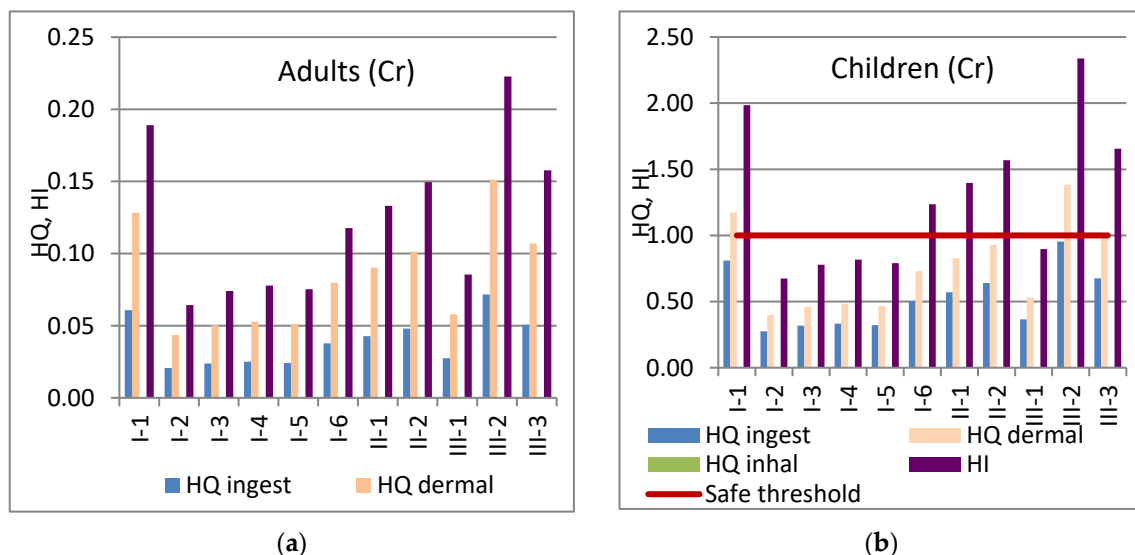
Figure 11. Health risk through ingestion, dermal contact and inhalation pathways: (**a**) Chromium exposure of adults; (**b**) Chromium exposure of children; (**c**) Cobalt exposure of adults; (**d**) Cobalt exposure of children.

4. Conclusions

This research represents the first comprehensive investigation in the Galati-Braila region, SE Romania, focusing on the elemental, mineralogical, and microstructural analysis of soil and three crop sections (leaves and grains/seeds of wheat, corn and sunflower) cultivated in the areas of Sendreni and Tulucesti, Galati County, and Vadeni, Braila County.

It is the first scientific endeavor to evaluate the bioaccumulation capacity of micro and macroelements in the plant tissues of wheat, corn, and sunflower using Bioaccumulation Factors (BFs) in the agroecosystems neighboring the Galati Iron and Steel Plant. Additionally, it contributes to the assessment of human health risks posed by topsoil dispersed particles.

The integrated analytical methods (HR-CS AAS, ATR-FTIR, SEM-EDX, PIGE) have proven to be valuable in identifying and quantifying environmental issues that affect the population residing near the industrial facility.

This work may serve as a foundational framework for initiating innovative agropedological and plant physiology studies in the specific agricultural and ecological context of the south-eastern region of Romania.

Appendix A

Table A1. Semi-quantitative EDX results of agricultural soil from Tulucesti and Sendreni (Galati county), and Vadeni (Braila county).

Elements	Tulucesti		Sendreni		Vadeni	
	0-5 cm	5-30 cm	0-5 cm	5-30 cm	0-5 cm	5-30 cm
	Average concentration (wt %)					
C	10.86	9.96	10.63	11.88	10.14	14.82
N	1.50	*	*	*	*	0.87
O	41.63	39.75	38.17	39.17	36.10	28.84
Na	0.45	0.38	0.58	0.39	0.40	0.62
Mg	1.32	1.54	1.31	1.46	1.07	1.03
Al	6.33	7.77	6.02	6.74	7.06	10.74
Si	23.83	22.60	22.44	20.84	25.28	26.27
P	0.26	0.24	0.10	0.15	0.26	0.16
S	0.09	0.02	0.09	0.10	0.19	0.04

Cl	0.07	*	*	*	*	*
K	2.59	3.33	1.63	1.77	3.57	3.43
Ca	3.58	3.64	4.67	6.26	1.69	2.69
Ti	0.55	0.55	0.43	0.55	0.65	0.88
V	*	*	*	0.20	*	*
Cr	0.23	*	0.35	0.19	0.49	*
Mn	0.27	0.47	0.40	0.51	0.67	*
Gd	*	1.46	1.33	0.87	1.59	*
Fe	4.04	5.08	4.02	5.07	5.52	8.35
Co	0.66	0.75	0.63	0.61	0.97	1.27
Ni	0.63	0.81	0.65	0.48	0.56	*
Cu	*	*	1.08	0.78	1.05	*
Zn	1.14	0.56	0.97	1.00	1.36	*
Ga	*	1.09	1.14	1.03	1.42	*
Hg	*	*	3.40	*	*	*
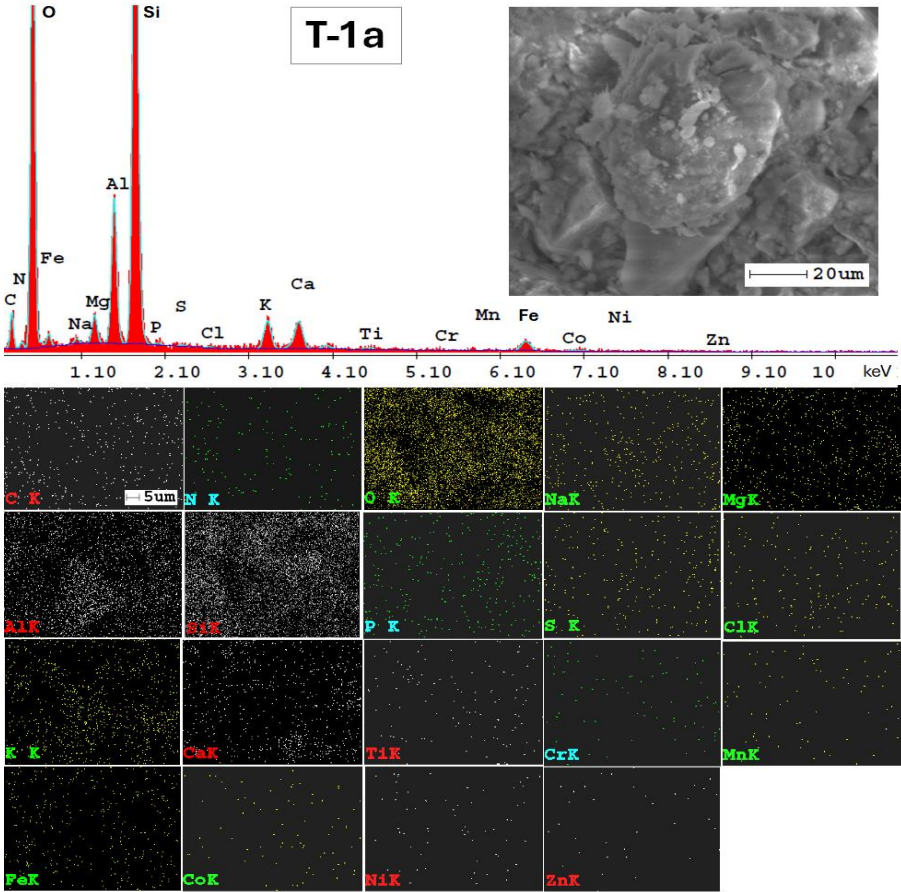
Figure A1. SEM-EDX spectrum of a soil sample and the elemental map distribution.

a)

b)

40

c)
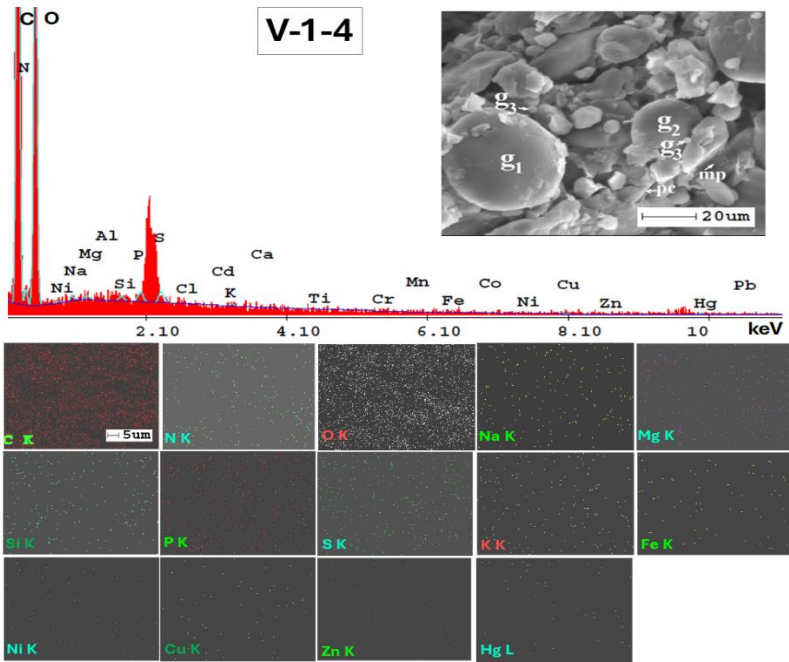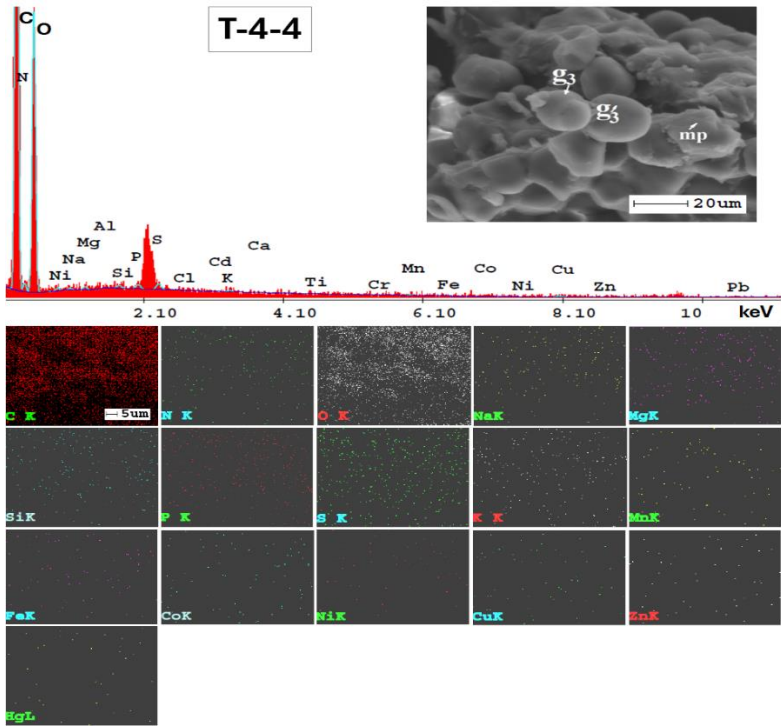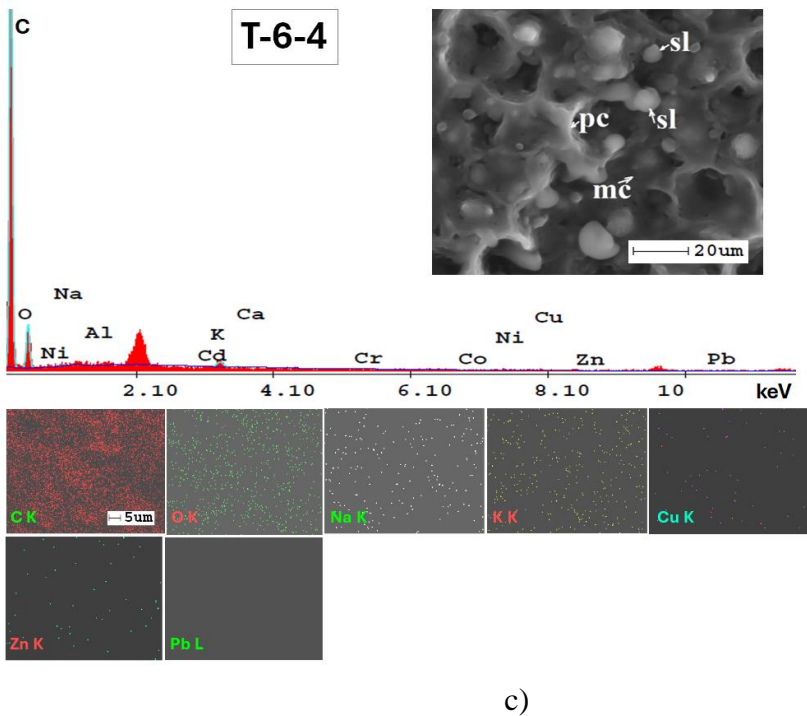
Figure A2. SEM-EDX spectra and elemental maps for selected vegetal compartments. a) SEM-EDX spectrum of *Triticum vulgare Vill.* caryposis and the elemental map distribution (large starch granule (g1), medium starch granule (g2), small starch granule (g3), protein matrix (mp), cell wall (pc); b) SEM-EDX spectrum of a *Zea mays L.* caryposis and the elemental map distribution (small starch granule (g3), protein matrix (mp)); c) SEM-EDX spectrum of cross-sectioned achenes of *Helianthus annus L.* and the elemental map distribution (lipid spherosomes (sl), cell membrane (mc), cell wall (pc)).

Table A2. Semi-quantitative EDX results for *Triticum vulgare Vill.* and *Zea mays L.* caryopsis, and *Helianthus annuus L.* achenes, collected from Tulucesti and Sendreni (Galati county), and Vadeni (Braila county).

Elements	*Triticum vulgare Vill.*	*Zea mays L.*	*Helianthus annuus L.*
	Average concentration (wt %)		
C	59.76	65.65	74.61
N	3.50	2.60	*
O	24.80	23.18	18.49
Na	0.10	0.08	0.16
Mg	0.20	0.22	*
Al	0.20	0.27	0.06
Si	0.10	0.07	*
P	0.60	0.48	*
S	0.40	0.33	*
Cl	0.10	0.03	*
K	*	0.04	0.15
Ca	0.40	0.21	1.93
Ti	*	0.04	1.46
V	*	0.03	*
Cr	0.10	0.03	0.16
Mn	0.10	0.14	*
Fe	0.20	0.27	*

41

Co	0.30	0.18	*
Ni	0.30	0.60	0.19
Cu	0.90	1.18	0.17
Zn	0.80	0.66	0.09
Pb	6.18	3.71	2.57
Hg	1.24	*	*

* not detected.

Author Contributions: Conceptualization, Antoaneta Ene and Sorina Simona Moraru; Data curation, Antoaneta Ene and Sorina Simona Moraru; Formal analysis, Alina Mihaela Ceoromila; Investigation, Antoaneta Ene, Sorina Simona Moraru, Dana Iulia Moraru, Ana Pantelica, Steluta Gosav and Alina Mihaela Ceoromila; Methodology, Antoaneta Ene, Sorina Simona Moraru, Dana Iulia Moraru, Ana Pantelica, Steluta Gosav and Alina Mihaela Ceoromila; Project administration, Antoaneta Ene; Resources, Antoaneta Ene and Ana Pantelica; Software, Sorina Simona Moraru and Steluta Gosav; Validation, Sorina Simona Moraru and Dana Iulia Moraru; Visualization, Steluta Gosav; Writing – original draft, Antoaneta Ene and Sorina Simona Moraru; Writing – review & editing, Antoaneta Ene, Sorina Simona Moraru, Dana Iulia Moraru, Ana Pantelica, Steluta Gosav and Alina Mihaela Ceoromila. All authors have read and agreed to the published version of the manuscript.

Institutional Review Board Statement: Not applicable.

Data Availability Statement: Data supporting reported results are available from the corresponding author upon request.

Conflicts of Interest: The authors declare no conflicts of interest.

References

1. Arbanas (Moraru), S.-S. Research on iron and steel works industry impact on soil edaphic and vegetal potential in the adjacent areas (Cercetări privind impactul activităţilor industriei siderurgice asupra potenţialului edafic and vegetal al solurilor din zonele adiacente – in Romanian). PhD Thesis, Dunarea de Jos University of Galati. Romania. 2022

2. Wang, Y.; Xu, W.; Wang, Z.; Zhu, Y. The Impact of Vegetation Roots on Shallow Stability of Expansive Soil Slope under Rainfall Conditions. *Appl. Sci.* **2023.** *13, 11619*. https://doi.org/10.3390/app132111619

3. Blum, W.E.H. Functions of Soil for Society and the Environment, *Rev. Environ. Sci. Bio* **2005.** *4, 75*. 75-79. https://doi.org/10.1007/s11157-005-2236-x

4. Trap, J.; Bonkowski, M.; Plassard, C.; Villenave, C.; Blanchart, E. Ecological importance of soil bacterivores for ecosystem functions, *Plant Soil* **2016.** *398*. 1-24. https://doi.org/10.1007/s11104-015-2671-6

5. Jakubus, M.; Bakinowska, E. The Effect of Immobilizing Agents on Zn and Cu Availability for Plants in Relation to Their Potential Health Risks. *Appl. Sci.* **2022**, *12*, 6538. https://doi.org/10.3390/app12136538

6. Costa, C.; Lia, F. Temporal Variations of Heavy Metal Sources in Agricultural Soils in Malta. *Appl. Sci.* **2022.** 12, 3120. https://doi.org/10.3390/app12063120

7. Zhou, B.; Zhang, T.; Wang, F. Microbial-Based Heavy Metal Bioremediation: Toxicity and Eco-Friendly Approaches to Heavy Metal Decontamination. *Appl. Sci.* **2023.** *13*, 8439. https://doi.org/10.3390/app13148439

8. Zhou, H.; Ouyang, T.; Guo, Y.; Peng, S.; He, C.; Zhu, Z. Assessment of Soil Heavy Metal Pollution and Its Ecological Risk for City Parks, Vicinity of a Landfill, and an Industrial Area within Guangzhou, South China. *Appl. Sci.* **2022.** 12, 9345. https://doi.org/10.3390/app12189345

9. Ene, A.; Sloată, F.; Frontasyeva, M. V.; Duliu, O. G.; Sion, A.; Gosav, S.; Persa, D. Multi-elemental Characterization of Soils in the Vicinity of Siderurgical Industry: Levels, Depth Migration and Toxic Risk. *Preprints* **2024**. 2024040668. https://doi.org/10.20944/preprints202404.0668.v1, accepted in *Minerals* on 25 May 2024

10. Order of the Minister of Water, Forest and Environmental Protection no. 184/21.09.1997 for the approval of the Procedure for the elaboration of environmental assessment, Official Monitor of Romania no. 303bis from 6.11.1997 (in Romanian). https://legislatie.just.ro/Public/DetaliiDocument/11971

11. Benton Jones Jr., J. Chapter 2. Field Sampling Procedures for Conducting a Plant Analysis. In *Handbook of Reference Methods for Plant Analysis*. *Tissue Tests. Let plant speak.* Kalra, Y.P. CRC Press. Taylor and Francis Group, USA, 1998; pp. 25-36.

12. SR ISO 11466:1999. Soil quality. Extraction of trace elements soluble in aqua regia.

13. SR 7184/13:2001. Soils. Determination of pH in water and saline suspensions (mass/volume) and in saturated paste.

14. STAS 7184/21-82. Soils. Determination of humus content.

15. SR EN ISO 10693:2014. Soil quality. Determination of carbonate content. Volumetric method.

16. Borlan, Z.; Rauta, C. (editors). *Methodology for agrochemical analysis of soils to establish the need for amendments and fertilizers*. *Methods of chemical analysis of soils*. Methods, guidance reports Series, ICPA. Bucharest. Romania. 1981; Volume I. Part I. (in Romanian).

17. SR ISO 11265+A1:1998. Soil quality. Determination of the specific electrical conductivity.

18. STAS 7184/7-87. Soils. Determination of mineral salts of 1:5 aqueous extract.

19. STAS 7184/10-79. Soils. Determination of granulometric composition.

20. SR ISO 11465:1998. Soil quality. Determination of dry matter and water content on a mass basis. Gravimetric method.

21. Caprita, F.-C.; Ene, A.; Cantaragiu Ceoromila, A. Valorification of Ulva rigida Algae in Pulp and Paper Industry for Improved Paper Characteristics and Wastewater Heavy Metal Filtration. *Sustainability* **2021.** *13, 19, 10763.* 1-23. https://doi.org/10.3390/su131910763

22. Wang, C.; Xu, D.; Li, Y.; Zhou, W.; Bian, P.; Zhang, S. Source and Migration Pathways of Heavy Metals in Soils from

23. an Iron Mine in Baotou City, China. *Minerals* **2024**. *14, 506.* 1-18. https://doi.org/10.3390/min14050506

24. Wu, C.; Sun, B.; Tian, M.; Cheng, X.; Liu, D.; Zhou, Y. Enrichment Characteristics and Ecological Risk Assessment of

25. Heavy Metals in a Farmland System with High Geochemical Background in the Black Shale Region of Zhejiang, China. *Minerals* **2024.** *14, 375.* 1-16. https://doi.org/10.3390/min14040375

26. Jaskuła, J.; Sojka, M.; Fiedler, M.; Wróżyński, R. Analysis of Spatial Variability of River Bottom Sediment Pollution with Heavy Metals and Assessment of Potential Ecological Hazard for the Warta River, Poland. *Minerals* **2021**, *11*, 327. 1-20. https://doi.org/10.3390/min11030327

27. Dou, C.; Cui, H.; Zhang, W.; Yu, W.; Sheng, X.; Zheng, X. Copper and Cadmium Accumulation and Phytoextraction Potential of Native and Cultivated Plants Growing around a Copper Smelter. *Agronomy* **2023**. *13*, 2874. 1-13. https://doi.org/10.3390/agronomy13122874

28. Yang, L.-Y.; Jiao, S.-L.; Wang, L.; Li, Y.-J.; Yang, M.; Feng, Y.-L.; Li, J.; Wei, Z.-X. Characteristics and Release Risk of Phosphorus from Sediments in a Karst Canyon Reservoir, China. *Appl. Sci.* **2024**. *14*, 2482. 1-13. https://doi.org/10.3390/app14062482

29. Ahmed, F.; Fakhruddin, A.N.M.; Toufick Imam, M.D.; Khan,. N.; Khan, T.A.; Rahman, M.M.; Abdulah, A.T.M. Spatial distribution and source identification of heavy metals pollution in roadside surface soil: a study of Dhaka Aricha highway, Bangladesh. *Ecol.Process.* **2016.** *5, 2.* 1-16. https://doi.org/10.1186/s13717-016-0045-5

30. Caeiro, S.; Costa, M.H.; Ramos, T.B.; Fernandes, F.; Silveira, N.; Coimbra, A.; Medeiros, G.; Painho, M. Assessing heavy metal contamination in Sado Estuary sediment: An index analysis approach. *Ecol. Indic.* **2005.** *5.* 151-169. http://dx.doi.org/10.1016/j.ecolind.2005.02.001

31. Sutherland, R.A. Bed sediment-associated trace metals in an urban stream, Oahu, Hawaii. *Environ. Geol.* **2000.** *39, 6.* 611-627. https://doi.org/10.1007/s002540050473

32. Awadh, S.M.; Al-Hamdani, J.A.JM.Z. Urban geochemistry assessment using pollution indices: a case study of urban soil in Kirkuk, Iraq. *Environ. Earth Sci.* **2019.** *78, 587.* 1-12. https://doi.org/10.1007/s12665-019-8615-3

33. Kowalska, J.B.; Mazurek, R.; Gąsiorek, M.; Zaleski, T. Pollution indices as useful tools for the comprehensive evaluation of the degree of soil contamination-A review. *Environ. Geochem. Health* **2018.** *Springer, 4.* 2395-2420. https://doi.org/10.1007/s10653-018-0106-z

34. Műller, G. Index of geoaccumulation in sediments of the Rhine River. *GeoJournal* **1969.** 108-118.

35. Nikolaidis, C.; Zafiriadis, I.; Constantinidis, T. Heavy Metal Pollution Associated with an Abandoned Lead-Zinc Mine in the Kirki Region, NE Greece. *Bull. Environ. Contam. Toxicol.* **2010.** *85*. 307-312. https://doi.org/10.1007/s00128-010-0079-9

36. Håkanson, L., An Ecological Risk Index for Aquatic Pollution Control: A Sedimentological Approach. *Water Res.* **1980.** *14.* 975-1101. https://doi.org/10.1016/0043-1354(80)90143-8

37. Pejman, A.; Bidhendi, G.N.; Ardestani, M.; Saeedi, M.; Baghvand, A. A new index for assessing heavy metals contamination in sediments: A case study. *Ecol. Indic.* **2015.** *58*. 365-373. https://doi.org/10.1016/j.ecolind.2015.06.012

38. El-Alfy, M.A.; El-Amier, Y.A.; El-Eraky, T.E. Land use/cover and eco-toxicity indices for identifying metal contamination in sediments of drains, Manzala Lake, Egypt. *Heliyon* **2020.** *6*. e03177. https://doi.org/10.1016/j.heliyon.2020.e03177

39. Long, E.R.; MacDonald, D.D.; Smith, S.; Calder, F.D. Incidence of Adverse Biological Effects Within Ranges of Chemical Concentrations in Marine and Estuarine Sediments. *Environ. Manage.* **1995.** *19, 1.* 81-97. https://doi.org/10.1007/BF02472006

40. Olowoyo, J.O.; van Heerden, E.; Fischer, J.L.; Baker, C. Trace elements in soil and leaves of Jacaranda mimosifolia in Tshwane area, South Africa. *Atmos. Environ.* **2010.** *44.* 1826-1830. https://doi.org/10.1016/j.atmosenv.2010.01.048

41. Mirecki, N.; Rukie Agič, R.; Šunić, L.; Milenković, L.; Ilić, Z. S. Transfer factor as indicator of heavy metals content in plants, *Fresenius Environ. Bul.* **2015.** PSP, 24, 11c. 4212-4219.

42. USEPA, California Department of Toxic Substances Control (DRSC), Office of Human and Ecological Risk (HERO), Human Health Risk Assessment (HHRA) Note number 1: Recommended DTSC Default Exposure Factors for Use in Risk Assessment at California Hazardous Waste Sites and Permitted Facilities, April 9, 2019.

43. https://dtsc.ca.gov/wp-content/uploads/sites/31/2022/02/HHRA-Note-1-April-2019-21A.pdf

44. Ackah, M. Soil elemental concentrations, geoaccumulation index, non-carcinogenic and carcinogenic risks in functional areas of an informal e-waste recycling area in Accra, Ghana. *Chemosphere* **2019.** *235.* 907-917.

45. https://doi.org/10.1016/j.chemosphere.2019.07.014

46. Zheng, X.; Zhao, W.; Yan, X.; Shu, T.; Xiong, Q.; Chen, F. Pollution Characteristics and Health Risk Assessment of Airborne Heavy Metals Collected from Beijing Bus Stations. *Int. J. Environ. Res. Public Health* **2015**. *12.* 9658-9671. https://doi.org/10.3390/ijerph120809658

47. Praveena, S.M.; Pradhan, B.; Aris, A.Z. Assessment of bioavailability and human health exposure risk to heavy metals in surface soils (Klang district, Malaysia). *Toxin Rev.* **2017.** *37, 3.* 196-205. https://doi.org/10.1080/15569543.2017.1350193

48. Slaboch, J.; Malý, M. Land Valuation Systems in Relation to Water Retention. *Agronomy* **2023.** *13, 2978.* 1-26. https://doi.org/10.3390/agronomy13122978

49. Zhang, Z.; Chen, X.; Qin, X.; Xu, C.; Yan, X. Effects of Soil pH on the Growth and Cadmium Accumulation in Polygonum hydropiper (L.) in Low and Moderately Cadmium-Contaminated Paddy Soil. *Land* **2023**. *12, 652.* https://doi.org/10.3390/land12030652

50. Xu, F.; Vaziriyeganeh, M.; Zwiazek, J.J. Effects of pH and Mineral Nutrition on Growth and Physiological Responses of Trembling Aspen (Populus tremuloides), Jack Pine (Pinus banksiana), and White Spruce (Picea glauca) Seedlings in Sand Culture. *Plants* **2020**. *9, 682.* 1-12. https://doi.org/10.3390/plants9060682

51. Adamczyk-Szabela, D.; Wolf, W.M. The Impact of Soil pH on Heavy Metals Uptake and Photosynthesis Efficiency in Melissa officinalis, Taraxacum officinalis, Ocimum basilicum. *Molecules* **2022.** *27, 4671.* 1-11. https://doi.org/10.3390/molecules27154671

52. Pikuła, D.; Stępień, W. Effect of the Degree of Soil Contamination with Heavy Metals on Their Mobility in the Soil Profile in a Microplot Experiment. *Agronomy* **2021.** *11, 878.* 1-11. https://doi.org/10.3390/agronomy11050878

53. Ahmad, I.; Malik, S.A.; Saeed, S.; Rehman, A.-u.; Munir, T.M. Phytoextraction of Heavy Metals by Various Vegetable Crops Cultivated on Different Textured Soils Irrigated with City Wastewater. *Soil Syst.* **2021**. *5, 35.* 1-13. https://doi.org/10.3390/soilsystems5020035

54. Arbanas (Moraru), S.-S.; Ene, A. Nutrient stocks study in agroecosystems located near the steel industry, Galati, Romania, *Annals of "Dunarea de Jos" University of Galati, Mathematics, Physics, Theoretical Mechanics, Fascicle II* **2020.** *43*(2). 82-93. 10.35219/ann-ugal-math-phys-mec.2020.2.02

55. Moraru, S.-S.; Ene, A.; Badila, A. Physical and Hydro-physical Characteristics of Soil in the Context of Climate Change. A Case Study in Danube River Basin, SE Romania. *Sustainability* **2020.** *12, 9174.* 1-26. https://doi.org/10.3390/su12219174

56. Kabata-Pendias, A. Chapter 3. Soils and Soils Processes. In *Trace elements in soils and plants*, 4th ed., CRC Press, Taylor and Francis Group. USA. 2011; 37-63.

57. Cullen, J.T.; Maldonado, M.T. Chapter 2. Biogeochemistry of Cadmium and Its Release to the Environment. In *Cadmium: From Toxicity to Essentiality*, Sigel. A.; Sigel. H.; Sigel. R.K.O (editors), Metal Ions in Life Science series, Springer. Germany. 2013; 11. 31-62. http://dx.doi.org/10.1007/978-94-007-5179-8_2

58. Salminen, R. (ed.); Demetriades, A.; Reeder, S. Geochemical Atlas of Europe, Part I - Background Information, Methodology and Maps, FOREGS. 2005. http://www.gtk.fi/publ/foregsatlas

59. Dumitru, M.; Dumitru, S.; Tanase, V.; Mocanu, V.; Manea, A.; Vrânceanu, N.; Preda, M.; Eftene, M.; Ciobanu, C.; Calciu, I.; Rasnoveanu, I. Soil Quality Monitoring in Romania, Sitech. Craiova, Romania. 2011. pp. 51-59.

60. Manea, A.; Dumitru, M.; Vrinceanu, N.; Eftene, A.; Anghel, A.; Vrinceanu, A.; Ignat, P.; Dumitru, S.; Mocanu, V. Soil heavy metal status from Maramureș county, Romania. In Proceeding GLOREP 2108 Conference. Timisoara, Romania. 15-17 November 2018.

61. Pantelica, A.; Freitas, M. do Carmo; Ene, A.; Steinnes, E. Soil pollution with trace elements at selected sites in Romania studied by instrumental neutron activation analysis, *Radiochim. Acta* **2013.** *101*. 45-50. https://doi.org/10.1524/ract.2013.1989

62. Order of the Minister of Water, Forest and Environmental Protection no. 756/3.11.1997 for the approval of the Regulation regarding the assessment of the environmental pollution, Official Monitor of Romania no. 303bis from 06.11.1997 (in Romanian). https://legislatie.just.ro/Public/DetaliiDocument/13572

63. City of Hope. Available online: https://www.cancercenter.com/risk-factors/fluoride (accesed on 14.04.2024)

64. Kumar, K.; Giri, A.; Vivek, P.; Kalaiyarasan, T.; Kumar, B. Effects of Fluoride on Respiration and Photosynthesis in Plants: An Overview, *JREST* **2017.** *2, 1*. 043-047. https://doi.org/10.17352/aest.000011

65. Bhat, N.; Jain, S.; Asawa, K.; Tak, M.; Shinde, K.; Singh, A.; Gandhi, N.; Gupta, V.V. Assessment of Fluoride Concentration of Soil and Vegetables in Vicinity of Zinc Smelter, Debari, Udaipur, Rajasthan, *J. Clin. Diagn. Res.* **2015.** 9(10): ZC63–ZC66. https://doi.org/10.7860%2FJCDR%2F2015%2F13902.6667

66. WHO - World Health Organization, Preventing disease through healthy environments. Inadequate or excess fluoride: A major public health concern, WHO/CED/PHE/EPE/19.4.5, (2019). Available online: https://apps.who.int/iris/handle/10665/329484 (accessed on 14.04.2024).

67. Bulgariu, D.; Scarlat, A. A.; Bulgariu, L.; Astefanei, D.; Ciobanu, S.C. Chapter VIII. Considerations for carbonate analysis in soils. In *Studies and research in geosciences.* Rusu. C.; Bulgariu. D. (editors.), "Al. I. Cuza" University. Iasi, Romania. 2018; Volume 2, 2018 (in Romanian).

68. Volkov, D.S.; Rogova, O.B.; Proskurnin, M.A. Organic matter and mineral composition of silicate soils: FTIR comparison study by photoacoustic, diffuse reflectance, and attenuated total reflection modalities, MDPI, *Agronomy* **2021.** *11, 9, 1879.* 1-30. https://doi.org/10.3390/agronomy11091879

69. Stoica, E.; Rauta, C.; Florea, N. (editors), *Methods of soil chemical analysis*, The Agricultural Technical Propaganda Office, Bucharest, Romania. 1986; pp. 412-418 (in Romanian).

70. Madejova, J.; Komadel, P. Baseline Studies of the Clay Minerals Society Source Clays: Infrared Methods, Clays Clay Miner. **2001.** *49, 5*. pp. 410-432. https://doi.org/10.1346/CCMN.2001.0490508

71. Müller, C. M.; Pejcic, B.; Esteban, L.; Delle Piane, C.; Raven, M.; Mizaikoff, B. Infrared Attenuated Total Reflectance Spectroscopy: An Innovative Strategy for Analyzing Mineral Components in Energy Relevant Systems, *Sci. Rep.* **2014.** *4, 6764.* 1-11. https://doi.org/10.1038/srep06764

72. Gosav, S.; Ene, A.; Aflori, M. Characterization and discrimination of plant fossils by ATR-FTIR, XRD and chemometric methods, *Rom. J. Phys.* **2019.** *64, 806*

73. Craciun, C, The study of some normal and abnormal montmorillonites by thermal analysis and infrared spectroscopy, *Thermochim. Acta* **1987.** *117*. 25-36. https://doi.org/10.1016/0040-6031(87)88097-8

74. Palacio, S.; Aitkenhead, M.; Escudero, A.; Montserrat-M, G.; Maestro, M.; Robertson, A.H.J. Gypsophile chemistry unveiled: Fourier Transform Infrared (FTIR) Spectroscopy provides new insight into plant adaptations to gypsum soils, *PloS ONE* **2014.** *9, 9, e107285*. 1-13. https://doi.org/10.1371/journal.pone.0107285

75. Mroczkowska-Szerszeń, M.; Orzechowski, M. Infrared spectroscopy methods in reservoir rocks analysis - semiquantitative approach for carbonate rocks, *NFG* **2018.** *ROK LXXIV, 11*. 802-8012. http://dx.doi.org/10.18668/NG.2018.11.04

76. Moraru, S.-S.; Ene, A.; Gosav, S. Study of the correlativity between parameters and mineralogy of contaminated agricultural soils, In Proceedings of the 19th International Multidisciplinary Scientific Conference on Earth & Planetary Science - SGEM Geoconference. Albena, Bulgaria, Section: Soils, 28th of June-07 of July 2019.

77. Sion, A.; Gosav, S.; Ene, A. ATR-FTIR qualitative mineralogical analysis of playground soils from Galati city, SE Romania, *Annals of "Dunarea de Jos" University of Galati, Mathematics, Physics, Theoretical Mechanics, Fascicle II* **2020.** *43*(2). 141-145. https://doi./10.35219/ann-ugal-math-phys-mec.2020.2.10

78. https://ptable.com/#Properties/Series (accessed on 26.05.2024)

79. Greger, M., Landberg, T., Vaculik, M.. Silicon influences soil availability and accumulation of mineral nutrients in various plant species, *Plants* **2018.** *7, 41*. 1-16. https://doi.org/10.3390/plants7020041

80. Tubana, B.S., Babu, T., Datnoff, L.E. A Review of Silicon in Soils and Plants and Its Role in US Agriculture: History and Future Perspectives, *Soil Sci.* **2016.** *181, 9-10*. 393-411. https://doi: 10.1097/SS.0000000000000179

81. Smical, A.I.; Hotea, V.; Oros, V.; Juhasz, J.; Pop, E. Studies on transfer and bioaccumulation of heavy metals from soil into lettuce, *EEMJ* **2008.** *7, 5*. 609-6015. http://dx.doi.org/10.30638/eemj.2008. 085

82. Krystofova, O.; Shestivska, V.; Galiova, M.; Novotny, K.; Kaiser, J.; Zehnalek, J.; Babula, P.; Opatrilova, R.; Adam, V.; Kizek, R. Sunflower Plants as Bioindicators of Environmental Pollution with Lead (II) Ions. *Sensors* **2009**. *9, 7*. 5040-5058. https://doi.org/10.3390/s90705040

83. Gopal, R.; Khurana, N. Effect of heavy metal pollutants on sunflower, *Afr. J. Plant Sci.* **2011.** *5, 9*. 531-536.

84. Dhiman, S.S.; Zhao. X.; Li, J.; Kim, D.; Kalia, V.C.; Kim, I.-W.; Kim, J.Y.; Lee, J.-K. Metal accumulation by sunflower (Helianthus annuus L.) and the efficacy of its biomass in enzymatic saccharification, *PloS One* **2017**. *12, 4, e0175845*. https://dx.doi.org/10.1371%2Fjournal.pone.0175845

85. Mani, D.; Sharma, B.; Kumar, C.; Pathak, N. Phytoremediation potential of *Helianthus annuus* L. in sewage-irrigated Indo-Gangetic alluvial soils, *Int. J. Phytoremediation* **2012.** *14, 3*. 235-246. https://doi.org/10.1080/15226514.2010.498844

86. Commision Regulation (EC) no. 1181/2006 of 19 December 2006 setting maximum levels of certain contaminants in foodstuffs, Official Journal of European Union. L364 20.12.2006 p. 5. Available on https://eur-lex.europa.eu/homepage.html

87. FAO/WHO, Codex Alimentarius - General standard for contaminants and toxins in food and feed, CXS 193-1995, (1995). Available on https://www.fao.org/fao-who-codexalimentarius (accessed on 19.05.2024)

88. Al-Othman, Z.A.; Ali, R.; Al-Othman, A.M.; Ali, J.; Habila, M.A. Assessment of toxic metals in wheat crops grown on selected soils, irrigated by different water sources, *Arab. J. Chem.* **2016.** *9*. S1555-S1562.

89. http://dx.doi.org/10.1016/j.arabjc.2012.006

90. Directive 2002/32/EC of the European Parliament and of the Council of 7 May 2002 on undesirable substances in animal feed - Council statement, Official Journal of European Union, Official Journal of the European Communities, Chapter 3. Volume 42. L140/10 30.5.2002. Available on http://data.europa.eu/eli/dir/2002/32/oj (accessed on 19.05.2024)

91. Yang, Y.; Nan, Z.; Zhao, Z. Bioaccumulation and translocation of cadmium in wheat (Triticum aestivum L.) and maize (Zea mays L.) from the polluted oasis soil of Northwestern China, *Chem Spec Bioavailab* **2014.** *26, 1*. 1-10. https://doi.org/10.3184/095422914X13888342841789

92. Alaboudi, K.A.; Ahmed, B.; Brodie, G. Phytoremediation of Pb and Cd contaminated soils by using sunflower (Helianthus annuus) plant, *Ann. Agric. Sci.* **2018.** *63, 1*. 123-127. https://doi.org/10.1016/j.aoas.2018.05.007

93. Tegegne, W.A. Assessment of some heavy metals concentration in selected cereals collected from local markets of Ambo City, Ethiopia, *J. Cereals Oilseeds* **2015.** *6, 2, 188B6F851564.* 8-13. https://doi.org/10.5897/ JCO15.0138

94. Shobha, N.; Kalshetty, B.M. Assessment of heavy metals in green vegetables and cereals collected from Jamkhandi local market, Bagalkot, India, *Rasayan J. Chem.* **2017.** *10, 1*. 124-135. http://dx.doi.org/10.7324/RJC.2017.1011575

95. Antoniadis, V.; Golia, E.E.; Lin, Y.-T.; Wang, S.-L., Shaeen, S.M. Soil and maize contamination by trace elements and associated health risk assessment in the industrial area of Volos, Greece, *Environ. Int.* **2019.** *124.* 79-88. https://doi.org/10.1016/j.envint.2018.12.053

96. Liang, J.; Chen, C.; Song, X.; Han, Y.; Liang, Z. Assessment of heavy metal pollution in soil and plants from Dunhua sewage irrigation area, *Int. J. Electrochem. Sci.* **2011.** *6, 11*. 5314-5324. https://doi.org/10.1016/S1452-3981(23)18409-4

97. Zehra, A.; Sahito, Z.A.; Tong, W.; Tang, L.; Hamid, Y.; Khan, M.B.; Ali, Z.; Naqi, B.; Yang, X. Assessment of sunflower germplasm for phytoremediation of lead-polluted soil and production of seed oil and seed meal for human and animal consumption, *J. Environ.l Sci.* **2020.** *87*. 24-38. https://doi.org/10.1016/j.jes.2019.05.031

98. https://specac.com/infrared-frequency-lookup/#frequencytool (accessed on 19.05.2024)

99. Demir, P.; Onde, S.; Severcan, F. Phylogeny f cultivated and wild wheat species using ATR-FTIR spectroscopy, *Spectrochim. Acta*, part A: Molecular and Biomolecular Spectroscopy **2015.** *135*. 757-763. https://doi.org/10.1016/j.saa.2014.07.025

100. Utami, S.N.H.; Suswati, D. Chemical and spectroscopy of peat from West and Central Kalimantan, Indonesia in relation to peat properties, *IJOEAR* **2016.** *2, 8*. 2454-1850.

101. Gorgulu, S.T.; Dogan, M.; Severcan, F. The characterization and differentiation of higher plants by Fourier Transform Infrared Spectroscopy, *Appl. Spectrosc.* **2007.** *61, 3*. 300-308. http://dx.doi.org/10.1366/000370207780220903

102. Heneen, W.K.; Brismar, K. Scanning electron microscopy of nature grains of rye, wheat and triticale with emphasis on grain shrivelling. *Hereditas* **1987.** 107. 147-162.

103. Shorstkii, I.A.; Zherlicin, A.G.; Li, P. Impact of pulse electric field and pulsed microwave treatment on morphological and structural characteristics on sunflower seed, *OCL* **2019.** *26, 47.* 1-7. https://doi.org/10.1051/ocl/2019048

104. Scheuer, P.M.; de Francisco, A.; de Miranda, M.Z.; Ogliari, P.J.; Torres, G.; Limberger, V.; Montenegro, F.M.; Ruffi, C.R.; Biondi, S. Characterization of Brazilian wheat cultivars for specific technological applications, *Food Sci. Technol* **2011.** *31, 3.* 816-826. https://doi.org/10.1590/S0101-20612011000300041